

International Spillover Effects of Air Pollution: Evidence from Mortality and Health Data*

Seonmin Will Heo

Koichiro Ito

UC Santa Barbara

University of Chicago and NBER

Rao Kotamarthi

Argonne National Laboratory

This version: September 26, 2024.

Abstract

International transboundary air pollution poses a significant threat to the global economy and health, yet conventional economic analyses seldom incorporate this phenomenon. By integrating transboundary particle trajectory data with individual-level mortality and emergency department visit records, we find that air pollution from China significantly increases mortality and morbidity in South Korea. We evaluate the spillover benefits of recent Chinese environmental regulations and find that a country's environmental policies could generate substantial hidden benefits for neighboring countries. Finally, we demonstrate that China's potentially strategic reductions in pollution could have undermined these benefits, highlighting the implications for additional gains through Coasian bargaining.

*Heo: University of California, Santa Barbara, 2127 North Hall, Santa Barbara, CA 93106 (e-mail: sheo@ucsb.edu). Ito: Harris School of Public Policy, University of Chicago, 1307 East 60th St., Chicago, IL 60637, and NBER (e-mail: ito@uchicago.edu). Kotamarthi: Argonne National Laboratory (E-mail: vrkotamarthi@anl.gov). We would like to thank Caleb Halvorson-Fried, Linnea Holy, Keisuke Ito and David Xu for excellent research assistance, and Severin Borenstein, Susanna Berkouwer, Marshall Burke, Judson Boomhower, Maureen Cropper, Olivier Deschênes, Dave Donaldson, Michael Greenstone, Danae Hernández-Cortés, Kelsey Jack, Ryan Kellogg, Nicolai Kuminoff, Shanjun Li, Kyle Meng, Joe Shapiro, Shaoda Wang, and seminar participants at UC Berkeley Energy Camp, the Griffin Conferences on Socioeconomic Effects of Air Pollution, and the Coase Project Conference for their helpful comments. We gratefully acknowledge financial support from the Global Energy Challenge by Argonne National Laboratory and the Energy Policy Institute at the University of Chicago and the Griffin Applied Economics Incubator on the Global Energy Challenge.

1 Introduction

A fundamental challenge of air pollution is its transboundary nature. Air pollution from a country is not confined to its borders and negatively affect neighboring nations. This also implies that a country’s environmental policy may yield international spillover benefits to other countries. International organizations such as the World Bank recognize air pollution’s international spillovers as a first-order problem in economic development ([World Bank, 2022](#)). However, the economics literature has generally not accounted for this spillover effect when evaluating the costs of air pollution and the benefits of environmental regulation. For example, the benefits of US environmental regulations are often estimated solely based on domestic impacts. Similarly, while recent ambitious environmental policies in China and India likely have substantial benefits to the environmental quality in neighboring countries, these effects are rarely considered in policy evaluations.

In this study, we examine the international spillover effects of air pollution and the extent to which conventional economic analysis understates the costs of air pollution and the benefits of environmental regulations. Our framework integrates recent advances in atmospheric science into econometric estimation. First, we obtain data on hourly particle trajectories from China to South Korea using the Hybrid Single-Particle Lagrangian Integrated Trajectory model (HYSPLIT).¹ Second, combining these particle trajectory data with hourly $PM_{2.5}$ data in China and South Korea, we estimate how transboundary $PM_{2.5}$ from China affects $PM_{2.5}$ in South Korea.² Finally, we connect these data with the universe of individual-level mortality data and emergency department visit data in South Korea to quantify the mortality and health impacts of transboundary air pollution.

We begin by presenting descriptive and visual evidence that transboundary air pollution from China plays a significant role in $PM_{2.5}$ levels in South Korea. In East Asia, the fall and winter seasons are dominated by prevailing west winds, called “the westerlies,” which bring consistent airflow from China to South Korea. During these seasons, we observe substantially higher $PM_{2.5}$ levels in the northwest region of South Korea compared to the southeast region. In contrast, these

¹Although outside the context of international spillovers, a growing number of recent economics studies use HYSPLIT to analyze air pollution ([Burke et al., 2023](#); [Fowlie, Rubin and Wright, 2021](#)).

² $PM_{2.5}$ refers to fine particles in the air that are two and one half microns or less in width.

regions have similar $\text{PM}_{2.5}$ levels in spring and summer. We use HYSPLIT to quantitatively confirm this relationship. Northwestern cities in South Korea—such as Incheon and Seoul—have trajectories originating in China more than half of the time during our sample period. By contrast, cities in the southeast, such as Busan, experience trajectories from China at a lower frequency.

We statistically estimate this relationship by regressing the hourly $\text{PM}_{2.5}$ levels in South Korean cities on the levels of hourly transboundary $\text{PM}_{2.5}$. We find that, on average, a $1 \mu\text{g}/\text{m}^3$ increase in transboundary $\text{PM}_{2.5}$ from China results in a $0.137 \mu\text{g}/\text{m}^3$ increase in $\text{PM}_{2.5}$ in South Korean cities. This estimate is robust and stable to the choice of fixed effects and control variables.

We then use the universe of individual-level mortality data in South Korea to estimate the mortality impact of transboundary air pollution. Our reduced-form estimates indicate that a $1 \mu\text{g}/\text{m}^3$ increase in transboundary $\text{PM}_{2.5}$ from China in the past 70 days results in an increase in hourly mortality in South Korea of 3.60 per billion people (or, an increase in annual mortality of 31.6 per million people). This effect implies a 0.6% increase in mortality with respect to a $1 \mu\text{g}/\text{m}^3$ increase in transboundary $\text{PM}_{2.5}$, relative to the baseline mortality rate for this population.

In addition to estimating the overall population's mortality impact, we also estimate the mortality effects on specific groups: the elderly (ages 65 and above), infants (ages below 1), and those who died from respiratory/cardiovascular diseases. The marginal effect on mortality is higher for infants (a 2.2% increase in mortality with respect to a $1 \mu\text{g}/\text{m}^3$ increase in transboundary $\text{PM}_{2.5}$ in the past 70 days) and those who succumbed to respiratory/cardiovascular diseases (a 1.1% increase in mortality). Our analysis also suggests that both instantaneous and lagged transboundary $\text{PM}_{2.5}$ levels affect mortality, although the lagged effects diminish after 70 days.

Using transboundary $\text{PM}_{2.5}$ levels from China as an instrumental variable (IV) for local $\text{PM}_{2.5}$ levels in South Korea, we also identify the effect of $\text{PM}_{2.5}$ on mortality. Our IV estimates indicate that a $1 \mu\text{g}/\text{m}^3$ increase in $\text{PM}_{2.5}$ in the past 70 days results in an increase in hourly mortality by 9.26 per billion people for the overall population. This effect implies an increase in annual mortality of 81.1 per million people and a 1.5% increase in mortality relative to the mean. The marginal effect as a percentage increase in mortality is greater for infants (a 5.8% increase) and

those with respiratory and cardiovascular diseases as the cause of death (a 2.9% increase).

Besides the mortality impact, air pollution may also increase morbidity (Barwick et al., 2018). In particular, short- and medium-run increases in air pollution are believed to affect acute symptoms of asthma and rhinitis (Eguiluz-Gracia et al., 2020; Kuiper et al., 2021). Thus, an increase in transboundary $PM_{2.5}$ from China to South Korea may increase such symptoms in the South Korean population. To investigate this issue, we collected data on the universe of emergency department (ED) visits in South Korea between 2013 and 2017 for patients who received medical treatment in the ED for atopic dermatitis, rhinitis, or asthma. We find that increases in transboundary $PM_{2.5}$ result in a greater number of ED visits for asthma and rhinitis but not for atopic dermatitis. The reduced-form results imply that a $1 \mu g/m^3$ increase in transboundary $PM_{2.5}$ from China to South Korea results in an increase in daily ED visits by 45.2 and 502.7 per billion people for asthma and rhinitis, respectively, which are 0.5% and 3.6% increases relative to their means.

Our results suggest that transboundary air pollution from China has substantial impacts on mortality and morbidity in South Korea. This finding implies that a country's environmental regulations may produce cross-country spillover benefits. To highlight this point, we examine an implication of a prominent environmental policy recently implemented in China known as “the war on pollution” (Greenstone, He, Li and Zou, 2021). Since 2014, the Chinese government has introduced a nationwide air pollution reduction program. Our data suggest that $PM_{2.5}$ levels in China had a long-run decline during our sample period, which resulted in a decline in transboundary $PM_{2.5}$ levels—the average level of transboundary $PM_{2.5}$ from China to South Korea declined by $9.63 \mu g/m^3$ in 2019 compared to 2015.

We quantify the spillover benefits of the Chinese environmental regulation for South Korea using our empirical findings and the value of a statistical life from the literature. We find that a $9.63 \mu g/m^3$ reduction in transboundary $PM_{2.5}$ levels resulted in a spillover benefit of \$2.80 billion per year for South Korea.³ This result suggests that the international spillover benefit of environmental regulation is economically substantial.

³The value is in 2019 US dollars. See footnote 22 for more details.

Finally, we investigate China’s potential strategic pollution reductions and their implications for Coasian bargaining. Several previous studies on water pollution find that a county may exploit international spillovers of water pollution and strategically allocate the flow of pollution in trans-boundary rivers (Sigman, 2002). To the best of our knowledge, the possibility of such strategic behavior has not yet been investigated for air pollution. We find suggestive empirical evidence of China’s strategic reductions in air pollution. During our sample period, the reduction in $PM_{2.5}$ levels was $9.29 \mu g/m^3$ in Chinese cities where most air pollution dispersed beyond the national border. This is lower than the nationwide average reduction ($14.07 \mu g/m^3$) and much lower than the reduction in Chinese cities where most air pollution remained within China ($18.32 \mu g/m^3$). This potential strategic pollution reduction implies that the international spillover benefits we find can be lower than those in a counterfactual scenario absent of this potential strategic decision. We show that the additional international spillover benefit of the war on pollution for South Korea could have been up to \$1.29 billion per year.

Our study builds on four strands of the literature. First, we provide a new framework that integrates recent advances in atmospheric science into econometric estimation with microdata on mortality and health. Previous economic studies use indirect measures of transboundary air pollution such as interactions between wind direction and air pollution or specific events including yellow dust and wildfires (Sheldon and Sankaran, 2017; Jia and Ku, 2019; Cheung, He and Pan, 2020). This is because it has been difficult to obtain direct measurements of transboundary air pollution. For example, Jia and Ku (2019) use an innovative research design based on the incidence of Asian dust to estimate the impact of air pollution spillover from China to South Korea. The authors note that “tracing winds from the vast area of China to a specific district within South Korea is difficult and such data do not exist.” For this reason, the study focuses on district-by-month-level analysis. To address this challenge, we use HYSPLIT and obtain hourly transboundary $PM_{2.5}$ data for every city in South Korea. This approach makes it possible to link city-by-hour-level transboundary air pollution data with the universe of mortality and ED visit data in South Korea.

Second, our study expands on the findings of recent studies that use detailed data on air pol-

lution, mortality, and health to estimate the mortality and health impacts of air pollution. For example, [Deryugina et al. \(2019\)](#) estimate the mortality effect of $\text{PM}_{2.5}$ on the elderly in the United States from 1999 to 2013 using Medicare data with wind direction as an instrumental variable. Both these papers and our study connect microdata on mortality or health outcomes with detailed data on air pollution. Our study differs from these previous studies in two key respects. First, our research focuses on the international spillover effects. Second, we use data on the direct measures of particle trajectories based on HYSPLIT rather than wind direction to trace pollution trajectories.

Third, we provide new evidence on the international spillovers of environmental externalities. In the economics literature, the primary focus of this topic has been water pollution in transboundary rivers ([Sigman, 2002](#)). Our findings suggest that this issue is important in the design of international environmental policies, not only for water pollution but also for air pollution.⁴

Finally, our framework benefits from recent advancements in atmospheric science. Many recent studies in atmospheric science use HYSPLIT or similar models to obtain particle trajectories ([Lee et al., 2013](#); [Oh et al., 2015](#); [Lee et al., 2017a](#); [Bhardwaj et al., 2019](#); [Han et al., 2021](#)). These studies, however, usually do not estimate the impacts of transboundary air pollution on mortality or other economic and health outcomes. We contribute to this literature by connecting transboundary air pollution data from HYSPLIT with microdata on mortality and health to shed light on the economic implications of international air pollution spillovers.

2 Data and Descriptive Evidence

2.1 $\text{PM}_{2.5}$ in South Korea and China

We obtain hourly $\text{PM}_{2.5}$ concentrations in Chinese cities from Berkeley Earth’s air pollution data. Berkeley Earth collects hourly $\text{PM}_{2.5}$ levels at the city level that are regionally interpolated with

⁴Our study is among recent papers that investigate this question for air pollution. For example, even though their focus is domestic air pollution spillovers—as opposed to international spillovers—[Monogan III et al. \(2017\)](#) and [Morehouse and Rubin \(2021\)](#) find evidence for strategic siting of polluting facilities within the United States.

real-time observations from ground-level monitors. We present monitor locations in Figure A.3.⁵

We collect hourly $PM_{2.5}$ concentrations in South Korean cities from the Korea Environment Corporation (KECO). The data contain hourly concentrations of pollutants such as $PM_{2.5}$, PM_{10} , SO_2 , CO , O_3 , and NO_2 . The National Institute of Environmental Research in South Korea collects data from 153 monitors, with records dating back to 2001. Although PM_{10} data have been collected since 2001, collection of $PM_{2.5}$ data only began in 2015 as part of the Clean Air Conservation Act (passed in October 2013). We show monitor locations in Figure A.4.⁶

Figure 1 provides suggestive evidence that transboundary air pollution from China may play a significant role in the $PM_{2.5}$ levels in South Korea. It shows the time-series variation in $PM_{2.5}$ levels in China and South Korea between January 2015 and December 2020. We split South Korea into two regions: northwest (i.e., regions closer to China) and southeast (i.e., regions relatively far from China) to examine how $PM_{2.5}$ levels in China correlate differently with $PM_{2.5}$ levels in the northwest and southeast regions in South Korea.

The figure suggests that $PM_{2.5}$ levels in China has persistently declined during our sample period. Many previous studies find that a large part of this reduction can be attributed to aggressive environmental regulation implemented in China, known as “the war on pollution” (Greenstone, He, Li and Zou, 2021). Our monitor-level data suggest that the reduction in $PM_{2.5}$ levels from 2015 to 2019 on average was $14.07 \mu\text{g}/\text{m}^3$ (unweighted) and $14.80 \mu\text{g}/\text{m}^3$ (population-weighted).

In addition, the level of $PM_{2.5}$ in China is almost always higher than that in South Korea and, in general, higher in fall and winter than in summer and spring. This is because heating in fall and winter is a major source of air pollution in China (Ito and Zhang, 2020). In East Asia, fall and winter are characterized by prevailing west winds, called “the westerlies.” In Figure A.2, we use wind data to show that this is in fact the case—in South Korea, the wind blows from west to east over 70% of the time in fall and winter. The wind speed is also higher in fall and winter than in spring and summer (Figure A.2). The combination of higher $PM_{2.5}$ levels in China and the seasonal westerlies could explain why systematic deviations in $PM_{2.5}$ levels exist between the

⁵The air pollution data are available at the Berkeley Earth website: <http://berkeleyearth.org>.

⁶Data are available at AirKorea, a webpage operated by KECO: <https://www.airkorea.or.kr/web>.

northwest and the southeast regions of South Korea only in fall and winter. The $\text{PM}_{2.5}$ levels are similar in the northwest and the southeast regions during spring and summer. By contrast, the northwest region has substantially higher $\text{PM}_{2.5}$ levels than the southeast region in fall and winter, when the $\text{PM}_{2.5}$ levels in China tend to be high and the area is prone to persistent westerlies.

While the visual analysis based on raw data in Figure 1 is informative, it neither controls for potential confounding factors nor provides direct information on transboundary air pollution. In the next section, we describe how we obtain such direct information and how we use our research design to control for potential confounding factors.

2.2 Transboundary Air Pollution from China to South Korea

Researchers in atmospheric science have recently developed several ways to obtain direct measures of transboundary air pollution. One of the state-of-the-art methods is the Hybrid Single-Particle Lagrangian Integrated Trajectory model (HYSPLIT) developed by the National Oceanic and Atmospheric Administration (NOAA) Air Resources Laboratory. HYSPLIT has been used in a variety of applications to describe atmospheric transport, dispersion, and deposition of pollutants. It can provide particle trajectories to determine the distance and locations to which particles travel.⁷

With meteorological data, HYSPLIT provides data on forward or backward pollution trajectories.⁸ The forward trajectories trace the movement of particles from a given point and time, while the backward trajectories trace the movement of particles backward in time from the arrival location. These two trajectories are useful for answering different sets of questions. For example, forward trajectories can be used to analyze the effect of emissions from a point source such as a factory or a volcano. On the other hand, backward trajectories help determine possible sources that

⁷Among atmospheric transport models, HYSPLIT provides tractable and reliable information on long-distance particle dispersion. We use HYSPLIT because our focus is the long-run dispersion of $\text{PM}_{2.5}$. An important limitation of our approach is that HYSPLIT does not allow us to study the chemical reactions of pollutants. One example of alternative models is AERMOD, which is a steady-state Gaussian-plume dispersion that can incorporate chemical reactions. However, at this time, it is only designed for measuring short-range particle dispersion up to 50 km. Incorporating chemical reactions in long-distance dispersion is an ongoing frontier research topic in atmospheric science, and we believe it is an important area of further research.

⁸For meteorological data, we use the NCEP/NCAR reanalysis data. Further details are available in [Appendix A](#).

might contribute to high levels of pollution in one area. We use backward trajectories in most of our analysis and forward trajectories in Section 4. We provide a detailed description of HYSPLIT and its application to our analysis in [Appendix A](#).

It is worth clarifying that HYSPLIT does not use any air pollution information when obtaining trajectories, and therefore, particle trajectories obtained by HYSPLIT are not endogenous to local pollution. HYSPLIT uses meteorological data to identify the trajectory of a particle from one location to another without using air pollution data.

In [Figure 2](#), we show a few HYSPLIT backward trajectories using Seoul and particular three hours as examples. For instance, the red line shows the backward trajectory of a particle that arrived in Seoul at 8 pm on June 15, 2015. HYSPLIT provides data on the particle trajectory’s longitude, latitude, and altitude every hour. For each city in South Korea, we obtain backward trajectories for every hour in our sample period. Each hourly backward trajectory starts from the destination city’s centroid and traces the particle trajectory backward. With this process, we obtain 6.57 million backward trajectories in total ($24 \text{ hourly trajectories} \times 365 \text{ days} \times 5 \text{ years} \times 228 \text{ cities in South Korea}$). While this is a computationally-intensive data collection, parallel computing allows us to obtain millions of trajectories in about a week.

In [Figure 3](#), we present how often South Korean cities have backward trajectories originating from China, by calculating the percentage of hours for which a city had trajectories originating from China in our sample period.⁹ The denominator is the total number of hours from January 1, 2015 to December 31, 2019, and the numerator is the total number of hours in which the backward trajectories came from China. The figure indicates substantial heterogeneity among South Korean cities. Cities in the northwest, such as Incheon and Seoul, have trajectories coming from China more than half of the time in our sample period. By contrast, cities in the southeast, such as Busan, less likely to have trajectories from China.

In [Figure 4](#), we show how often Chinese cities have trajectories that arrive in any South Korean city. For each city in China, we calculate the ratio of particles traveling to South Korea—the

⁹We consider that a backward trajectory comes from China if the trajectory is from the interior of China’s borders at a height below 1 km.

denominator is the total number of hours from January 1, 2015 to December 31, 2019, and the numerator is the total number of hours in which a trajectory went from the city in China to any South Korean city. We find higher fractions of trajectories coming from the northeastern part of mainland China, particularly Liaoning province owing to the persistent west-blowing wind in this region (the westerlies) and the proximity to South Korea. This figure illustrates that transboundary air pollution from these regions is more likely to affect South Korean cities.

We also investigate how long each trajectory takes to travel from China to South Korea. For each trajectory from China to South Korea, we observe how many hours it took to move from the last grid point in China to the city in South Korea. We present the distribution of this duration in Figure A.5. The median is 38 hours, and there is substantial variation in the duration (the 25th and 75th percentiles are 22 and 69 hours respectively). This substantial heterogeneity suggests that it is important to obtain direct information on each trajectory from HYSPLIT and that commonly-used indirect approaches (e.g. using average air pollution in China one or two days ago as a proxy for transboundary air pollution today) may not be able to accurately capture real-time transboundary air pollution.¹⁰

We construct a variable $\text{TransboundaryPM}_{ct}$ based on the hourly backward trajectory data and $\text{PM}_{2.5}$ data in China. For each hour t in city c in South Korea, we observe whether the backward trajectory comes from China. If the trajectory does not come from China, we define $\text{TransboundaryPM}_{ct}$ as zero as the focus of our study is transboundary air pollution from China. When the trajectory comes from China, we collect its origin's location and time. By merging this information with city-level data on hourly $\text{PM}_{2.5}$ in China, we can obtain $\text{PM}_{2.5}$ levels at the origin of the trajectory. We set this value to be $\text{TransboundaryPM}_{ct}$. For example, suppose that a pollution trajectory travels for 24 hours from Beijing to Seoul and arrives at hour t . In that case, $\text{TransboundaryPM}_{ct}$ equals the $\text{PM}_{2.5}$ level in Beijing in hour $t - 24$.¹¹

¹⁰This distribution also suggests that most trajectories from China to South Korea travel less than 100 hours. For this reason, we use 200 hours as the maximum run-time to obtain relevant trajectories for our analysis.

¹¹For trajectories that passed through multiple cities in China, we consider two approaches to calculate $\text{TransboundaryPM}_{ct}$. The first approach is to incorporate air pollution from every relevant Chinese city by calculating the average of $\text{PM}_{2.5}$ levels from all Chinese cities that the trajectory passed through. The second approach is to use $\text{PM}_{2.5}$ levels in the last Chinese city that the trajectory passed through before arriving in South Korea. We find

The particle trajectory data by itself does not uncover how transboundary air pollution affects local air pollution in South Korea. Our idea is that we can empirically estimate this relationship by regressing local hourly $\text{PM}_{2.5}$ levels in South Korean cities c in hour t on $\text{TransboundaryPM}_{ct}$. In section 3.1, we find a strong systematic relationship between these two variables and demonstrate that this relationship is robust to the inclusions of various fixed effects and control variables.¹²

2.3 Mortality in South Korea

We collect mortality data from the MicroData Integrated Service (MDIS), which is operated by Statistics Korea, South Korean government’s national statistical agency. The microdata include the universe of individual-level mortality information from January 1997 to December 2019, including each individual’s date and hour of death, age, sex, city of death, and cause of death.¹³

2.4 Emergency Department Visits in South Korea

We obtain data on emergency department (ED) visits in South Korea between 2013 and 2017 for patients admitted due to atopic dermatitis, rhinitis, or asthma. The National Health Insurance Service (NHIS) in South Korea provides data on all ED admissions at the district and daily level. The data are representative of the whole South Korean population, as nearly all eligible citizens are beneficiaries of this national insurance policy.

that these two approaches produce virtually identical results. We use the first approach for our main results and report the results with the second approach in the appendix, Tables A.3 through A.6.

¹²In the HYSPLIT, we need to specify the starting height of the backward trajectories. We follow the literature in atmospheric science to use 500 meters for our main results and examine their robustness in Table A.10. The results in Table A.10 suggest that they are robust to heights over 500 meters and that the Kleibergen-Paap rk Wald F-statistic is highest with 500 meters. Similarly, we need to specify the heights of the trajectories in China (the height at the origin of the backward trajectory) to determine the origin of the trajectory. Studies in atmospheric science use a height of 1,000 meters, and we find that indeed this height at the origin produces the highest Kleibergen-Paap rk Wald F-statistic in our first stage regression.

¹³Data are available at MDIS: <https://mdis.kostat.go.kr>.

2.5 Other Data and Summary Statistics

We obtain monitor-level hourly South Korean meteorological data from January 2001 to December 2019 from the Korea Meteorological Administration. This dataset includes wind speed and direction, temperature, and precipitation levels. We show the monitor locations in Figure A.4.

To create maps, we obtain shapefiles for China from the United Nations Office for the Coordination of Humanitarian Affairs and OSM-Boundaries, and a shapefile for South Korea from Geoservice Inc., a research institute that provides technology on geographic information systems (GIS), three-dimensional visualization, and deep learning.¹⁴

Table 1 provides summary statistics. The average $\text{PM}_{2.5}$ level in our sample period is 45.05 $\mu\text{g}/\text{m}^3$ in China and 24.99 $\mu\text{g}/\text{m}^3$ in South Korea. The mortality data suggest that approximately a quarter of mortality in South Korea is due to respiratory or cardiovascular illnesses.

3 Empirical Analysis and Results

In this section, we begin by estimating the first-stage regression in section 3.1 to estimate the impact of transboundary air pollution on local air pollution in South Korea. We then estimate the reduced-form in section 3.2 to identify the impact of transboundary air pollution on mortality in South Korea. Finally, in section 3.3, we run the instrumental variable (IV) estimation to estimate the effect of local air pollution on mortality in South Korea.

3.1 First-stage Regression

We use PM_{ct} to denote hourly $\text{PM}_{2.5}$ levels in South Korean city c in hour t and $\text{TransboundaryPM}_{ct}$ to denote the level of hourly transboundary $\text{PM}_{2.5}$ that reached city c in hour t . In the first-stage regression, we estimate the impacts of transboundary air pollution from China on local air pollution

¹⁴These shapefiles are available online at <https://data.humdata.org/dataset/china-administrative-boundaries>. and <http://www.gisdeveloper.co.kr>.

in South Korea by running the ordinary least squares (OLS) regression for the following equation:

$$\text{PM}_{ct} = \alpha \text{TransboundaryPM}_{ct} + X_{ct}\gamma + u_{ct}, \quad (1)$$

where X_{ct} is a vector of control variables for city c and hour t , and u_{ct} is the error term. We include a set of control variables to control for potential confounding factors such as seasonality and weather. In the most restrictive specification, we include city-by-year-by-month fixed effects, city-by-day of week fixed effects, city-by-rainfall quartile fixed effects, and city-by-temperature quartile fixed effects. The identifying assumption is that the error term is uncorrelated with transboundary air pollution given the control variables and fixed effects in the equation. To account for both the potential serial correlation and spatial correlation of the error term, we use two-way cluster-robust standard errors at the city and hour levels ([Cameron et al., 2011](#)).

In Figure 5, we provide a binned scatter plot of PM_{ct} against $\text{TransboundaryPM}_{ct}$ to non-parametrically examine the relationship between these two variables. Panel A shows the binned scatter plot of the raw data without controls. We use $1 \mu\text{g}/\text{m}^3$ of $\text{TransboundaryPM}_{ct}$ as the bin size to calculate the average PM_{ct} level for each bin. The figure suggests a strong relationship between the two variables. In Panel B, we residualize these variables by city-by-year-by-month fixed effects, city-by-day of week fixed effects, city-by-rainfall quartile fixed effects, and city-by-temperature quartile fixed effects. We find that the relationship between PM_{ct} levels and $\text{TransboundaryPM}_{ct}$ levels is robust to these controls. Recall that HYSPLIT does not use any air pollution information to obtain particle trajectories, and therefore, the positive relationship shown in Figure 5 is not mechanical from HYSPLIT.

Table 2 shows the regression results of Equation (1). The results suggest that the estimate is robust and stable to the choice of fixed effects and control variables. The coefficient in Column 4 implies that, on average, a $1 \mu\text{g}/\text{m}^3$ increase in transboundary $\text{PM}_{2.5}$ from China results in a $0.137 \mu\text{g}/\text{m}^3$ increase in $\text{PM}_{2.5}$ in South Korean cities. The Kleibergen-Paap rk Wald F-statistic is 3,953, suggesting that there is a strong first-stage relationship between these two variables.

3.2 Reduced-form Estimation

To identify the impact of transboundary air pollution from China on mortality in South Korean cities, we estimate the following equation by OLS:

$$\text{Mortality}_{ct} = \sum_{j=0}^J \beta_j \text{TransboundaryPM}_{c,t-j} + X_{ct}\gamma + u_{ct}, \quad (2)$$

where Mortality_{ct} is the hourly mortality (deaths per billion people) in city c in hour t . We include both the concurrent ($j = 0$) and lagged ($j > 0$) transboundary air pollution to estimate β_j for $j = 1, \dots, J$. These coefficients estimate the short- and medium-run effects of transboundary air pollution on mortality. We include the same set of fixed effects and control variables as the ones included in the most restrictive specification (the final column) of Table 2 and use two-way cluster-robust standard errors at the city and hour levels.¹⁵

Table 3 shows the estimation results of Equation (2). In Panel A, we include the average of hourly transboundary $\text{PM}_{2.5}$ levels from China in the past 70 days to estimate the average effect of instantaneous and lagged transboundary $\text{PM}_{2.5}$ levels.¹⁶ The estimate for the overall population (in the final column) suggests that a $1 \mu\text{g}/\text{m}^3$ increase in transboundary $\text{PM}_{2.5}$ from China in the past 70 days results in an increase in hourly mortality of 3.60 per billion people in South Korea. Because the average hourly mortality is 618 per billion people in our sample, this marginal effect indicates a 0.6% increase in mortality with respect to a $1 \mu\text{g}/\text{m}^3$ increase in transboundary $\text{PM}_{2.5}$. In the final row of the table, we also show the implied marginal effect on annual mortality per million people. For the overall population, our estimate implies that a $1 \mu\text{g}/\text{m}^3$ increase in transboundary $\text{PM}_{2.5}$ in the past 70 days results in a 31.6 per million people increase in annual mortality.

In addition to the overall population, we also provide results for the elderly (ages 65 and above), infants (ages below 1), and those who die from respiratory/cardiovascular diseases. The marginal effect on mortality is higher for infants (a 2.2% increase in mortality with respect to $1 \mu\text{g}/\text{m}^3$

¹⁵In Table A.8, we show that our results are robust to the choice of different control variables and fixed effects.

¹⁶We show the results with the average of hourly transboundary $\text{PM}_{2.5}$ from China in the past 70 days in Panel A because we find that the lagged effects decay after 70 days in Panel B.

increase in transboundary $PM_{2.5}$) and those who succumbed to respiratory/cardiovascular diseases (a 1.1% increase in mortality).

In Panel B, we estimate the weekly lagged effects of transboundary $PM_{2.5}$ on mortality. We include a set of 7-day average hourly transboundary $PM_{2.5}$ levels from China. We find that transboundary air pollution that arrived in the past 14-63 days tends to have the largest partial effects on mortality, although pollution that arrived in the past 0-14 days also has significant effects. This effect decays as we consider lagged effects beyond 63 days and becomes statistically insignificant. This finding is consistent with the medium-run mortality effect of $PM_{2.5}$ found in the literature. For example, although the context is different from international air pollution spillover effects, [Deryugina, Heutel, Miller, Molitor and Reif \(2019\)](#) find that exposure to $PM_{2.5}$ has medium-run effects on mortality for Medicare recipients in the United States but these lagged effects diminish over time.¹⁷

In Figure 6, we visualize these weekly lagged effects and 95% confidence intervals. These weekly lagged effects are useful for examining the possibility of the “harvesting effect” frequently discussed in the literature ([Deschênes and Moretti, 2009](#)). The harvesting effect implies that air pollution may not cause more total deaths but only cause forward displacement of mortality. That is, air pollution may only result in the death of the sick who would have died a few days later even in the absence of air pollution. Therefore, previous studies suggest that researchers estimate either the longer-run average effect (such as our Panel A) or the series of lagged effects jointly with the instantaneous effect (such as our Panel B).

If there is a substantial harvesting effect, we would observe positive effects in shorter lags followed by negative effects in longer lags, creating a U-shaped line in Figure 6. Our estimation results, however, show positive and significant effects in all the lags for the past 70 days, resulting in an inverted U-shaped line. This evidence suggests that the harvesting effect is unlikely to be substantial in our context.

¹⁷[Deryugina, Heutel, Miller, Molitor and Reif \(2019\)](#) note, “the increase in the effect of a 1-day shock appears to level off after about 14 days, suggesting that the effects of acute exposure do not cause additional deaths beyond this point.”

3.3 Instrumental Variables Estimation

Figure 5 and Table 2 show a strong first-stage relationship between transboundary $\text{PM}_{2.5}$ traveling from China to South Korea and $\text{PM}_{2.5}$ levels in South Korea. This suggests that we could use transboundary $\text{PM}_{2.5}$ levels as an instrument for local $\text{PM}_{2.5}$ levels to estimate the effect of $\text{PM}_{2.5}$ on mortality in South Korea. The exclusion restriction assumption required for this instrumental variable (IV) estimation is that given the set of control variables included in the estimation, transboundary $\text{PM}_{2.5}$ levels affects mortality only through local $\text{PM}_{2.5}$ levels.

We estimate the following equation using the IV regression:

$$\text{Mortality}_{ct} = \sum_{j=0}^J \phi_j \text{PM}_{c,t-j} + X_{ct}\gamma + u_{ct}. \quad (3)$$

We use $\text{TransboundaryPM}_{c,t-j}$ as an instrumental variable for $\text{PM}_{c,t-j}$, include the same set of fixed effects and control variables included in Equation (2), and use two-way cluster-robust standard errors at the city and hour levels.¹⁸

Table 4 presents the estimation results of Equation (3). The last column of Panel A indicates that a $1 \mu\text{g}/\text{m}^3$ increase in $\text{PM}_{2.5}$ in the past 70 days results in a 9.26 per billion people increase in hourly mortality for the overall population. This implies a 81.1 per million people increase in annual mortality and a 1.5% increase in mortality relative to the mean. The marginal effect in terms of a percentage increase in mortality is larger for infants (a 5.8% increase) and those who die from respiratory/cardiovascular diseases (a 2.9% increase).

Our reduced-form and IV estimates provide new evidence on the mortality impact of transboundary air pollution. We can compare our IV estimate to recent estimates of the mortality impacts of $\text{PM}_{2.5}$ in other contexts and discuss what makes these estimates similar or different. For example, [Deryugina, Heutel, Miller, Molitor and Reif \(2019\)](#) estimate the mortality effect of $\text{PM}_{2.5}$ for the elderly in the United States from 1999 to 2013 using the Medicare data with wind direction as an instrument. They find that a $1 \mu\text{g}/\text{m}^3$ increase in $\text{PM}_{2.5}$ exposure for one day causes

¹⁸We show that our results are robust to the choice of different control variables and fixed effects in Table A.9.

0.69 additional deaths per million elderly individuals over a three-day window that spans the day of the increase and the following two days. Panel B in our Table 4 suggests that the instantaneous marginal effect of $PM_{2.5}$ on the elderly is a 2.67 per billion people increase in hourly mortality, which implies a 0.19 per million people increase in three-day mortality.¹⁹ This implies that the magnitude of our IV estimate is similar to but slightly smaller than the IV estimate in [Deryugina, Heutel, Miller, Molitor and Reif \(2019\)](#). There are several possible explanations for this difference. First, the two studies use different instrumental variables and thus estimate different local average treatment effects ([Angrist and Imbens, 1995](#)). Second, the elderly in South Korea are known to have fewer underlying health conditions than the Medicare population in the United States, which could make them relatively less vulnerable to exposure to $PM_{2.5}$.²⁰

3.4 Mortality Impacts by Age Group

The impact of air pollution on mortality can differ substantially across age groups. This heterogeneity is important to quantify for our analysis of policy implications in Section 4. To estimate the heterogeneous effects of transboundary air pollution on mortality across ages, we divide our mortality data into age groups and estimate Equations (2) and (3) separately for each group.

In Table 5, we find that the mortality impact of transboundary air pollution is statistically and economically significant for infants and individuals over 30 years of age and insignificant for individuals aged 1–29 years. Note that the baseline mortality is low for those between 1–29 years, which could make statistically detecting the impact relatively more challenging.

The marginal effect on mortality in terms of percentage increases relative to the group’s baseline mortality level in each group is the largest for infants. However, the marginal effect in terms of increased death counts per billion people is higher for the elderly. We incorporate this heterogeneity in our analysis of policy implications in Section 4. Note that the IV estimates (Panel B) are

¹⁹This is because $2.67 \cdot 24 \cdot 3/1000 = 0.19$.

²⁰Another possibility is that the harmfulness of $PM_{2.5}$ exposure can differ between two locations because the toxicity of the small particles could vary. For example, [Hsiang, Lee and Wilson \(2022\)](#) find empirical evidence that supports this possibility.

larger than the OLS estimates (Panel A), because the first-stage coefficient on the transboundary air pollution (Table 2) is less than one.

3.5 Impacts on Emergency Department Visits

In addition to its impact on mortality, air pollution may also increase morbidity (Barwick et al., 2018). In particular, the short- and medium-run increases in air pollution are believed to influence the acute symptoms of asthma and rhinitis (Eguiluz-Gracia et al., 2020; Kuiper et al., 2021). Thus, the increase in transboundary PM_{2.5} traveling from China to South Korea might cause such symptoms to be more prevalent in the South Korean population.

In Table 6, we test this hypothesis using data on daily emergency department (ED) visits. The outcome variable is the number of ED visits by diagnosis at the city-day level. We use the same specification as Panel A in Tables 3 and 4 to estimate the reduced-form and IV regressions. Because seasonal pollen (oak, pine, and weed) is also known to be related to ED visits in South Korea, we include these three variables as additional controls in our estimation.

Results in Table 6 suggest that increases in transboundary PM_{2.5} levels result in increased ED visits for asthma and rhinitis. We do not find such an impact for atopic dermatitis. The reduced-form results imply that a 1 $\mu\text{g}/\text{m}^3$ increase in transboundary PM_{2.5} concentrations traveling from China to South Korea results in increases in daily ED visits of 45.2 and 502.7 per billion people for asthma and rhinitis, respectively, which are 0.5% and 3.6% increases relative to the means.

One way to quantify the economic costs of these increased ED visits is to calculate the direct medical costs of these visits. Kim et al. (2010) and Lee et al. (2017b) show that the average direct cost of an ED visit in South Korea is \$268 for asthma and \$64.91 for rhinitis. With these estimates, our findings imply that a 10 $\mu\text{g}/\text{m}^3$ increase in transboundary PM_{2.5} levels results in increases in South Korea's annual direct medical costs by \$2.29 million and \$6.17 million from increased ED visits for asthma and rhinitis, respectively.²¹

²¹Panel A in Table 6 implies that a 10 $\mu\text{g}/\text{m}^3$ increase in transboundary PM_{2.5} results in an additional 165 annual ED visits for asthma and 1,835 visits for rhinitis, per million people. Multiplying this by South Korea's population (51.76 million in 2019), the nationwide estimated total costs are \$2.29 million for asthma and \$6.17 million for asthma.

3.6 Avoidance Behavior

To prevent harm to public health, South Korean municipalities can issue alerts when air pollution reaches unhealthy levels. In this section, we examine whether these pollution alerts help mitigate the mortality impacts of transboundary air pollution by inducing avoidance behavior.

Municipalities issue an advisory alert when the average hourly $\text{PM}_{2.5}$ level exceeds $75 \mu\text{g}/\text{m}^3$ for two consecutive hours. They lift the alert when this average drops below $35 \mu\text{g}/\text{m}^3$. Pollution alerts are announced through mass media, government websites, text messages, and mobile applications. SMS notifications inform residents of the pollution alert issuance and encourage them to avoid strenuous outdoor activities. For each city and hour, we collected data on whether there was an air pollution alert.

In Table 7, we calculate the average of hourly alerts for the previous 70 days interacted with the average levels of transboundary air pollution for the same time frame. The negative coefficients on the interaction term suggest that air pollution alerts indeed mitigate the mortality impact of transboundary air pollution that we find in Table 3. These effects are statistically significant for the overall population and elderly but imprecise for infants and those with respiratory and cardiovascular diseases.

4 Policy Implications

4.1 International Spillover Benefits of Environmental Regulation

Our empirical findings suggest that transboundary air pollution from China has substantial impacts on mortality in South Korea. A key policy implication is that a country's environmental regulation may have an international spillover effect on citizens in other countries. As we discussed in the introduction, this spillover effect has not been incorporated in economic analysis of environmental regulation in the economics literature.

These estimates are in 2019 US dollars.

To highlight this point, we consider an implication of a prominent environmental policy recently implemented in China, known as “the war on pollution” (Greenstone, He, Li and Zou, 2021). In 2014, the Chinese government began to roll out a nationwide air pollution reduction program. As shown in Figure 1, our data suggest that $PM_{2.5}$ levels in China exhibited a long-run decline during our sample period. This reduction also resulted in a decline in transboundary $PM_{2.5}$ traveling from China to South Korea. Based on the data we obtained from HYSPLIT, we find that the annual average level of transboundary $PM_{2.5}$ from China to South Korea declined by $9.63 \mu\text{g}/\text{m}^3$ during our sample period (2015–2019).

We quantify South Korea’s economic benefit from this reduction in transboundary $PM_{2.5}$ levels based on the following procedure. Table 5 provides the age-specific reduced-form effects of transboundary $PM_{2.5}$ levels on mortality. We use these coefficients to calculate the benefit from a $9.63 \mu\text{g}/\text{m}^3$ reduction in transboundary $PM_{2.5}$ levels on mortality in each age group in South Korea. We then use the value of a statistical life (VSL) in the literature to obtain implied economic values arising from reductions in mortality. Working on the age-specific estimates—as opposed to using the average estimate—is important for two reasons. First, as we find in Table 5, the mortality effects of $PM_{2.5}$ are heterogeneous across age groups. Second, the VSL can differ across age groups as noted by Murphy and Topel (2006).

To our knowledge, no previous studies provide age-specific VSLs for South Korea. We find three economic studies that estimate South Korea’s average VSL. Therefore, we make the following assumptions to obtain age-specific VSL estimates. We calculate an average of the VSL estimates for South Korea from three studies in the literature (Shin and Joh, 2003; Kim et al., 2003; Lee et al., 2011). This average VSL is \$511,000 in 2019 US dollars.²² We then use the method developed in Murphy and Topel (2006) to obtain VSL estimates for each age group.²³ We

²²The VSL estimates in Shin and Joh (2003), Kim et al. (2003), and Lee et al. (2011) are 466, 463, and 277 million, respectively, in South Korean won. We use the Consumer Price Index (CPI) in South Korea—with values of 71.50, 73.11, 88.08, and 115.16 for the years 1999, 2000, 2006, and 2019, respectively—and the 2019 exchange rate (1165.36 KRW to 1 USD) to convert them to US dollars in 2019. These values are \$630,000, \$520,000, and \$383,000 in 2019 US dollars, respectively.

²³Figure 3 in Murphy and Topel (2006) shows the values of remaining lives at each age for the US population. We assume that the curvature of these age-specific values can be applied to the South Korean population and scale the function by the ratio of South Korea’s VSL to the US’s VSL in Murphy and Topel (2006).

present the age-specific VSLs obtained from this approach in Table A.13.

In Table 8, we present the result of our calculation in the first row. We find that a $9.63 \mu\text{g}/\text{m}^3$ reduction in transboundary $\text{PM}_{2.5}$ traveling from China to South Korea implies an economic benefit of \$2.80 billion per year for South Korea based on avoided mortality. This benefit represents 2.07% of the nation’s healthcare spending in 2019. On a per capita basis, the annual spillover benefit amounts to \$54 per capita, compared to the annual national healthcare expenditure of \$2,632 per person. This result suggests that the international spillover benefit of environmental regulation is economically substantial. The overall spillover benefit can be even larger than our estimate because our calculation does not include other potential benefits such as reductions in morbidity costs and negative effects on productivity and educational outcomes (Chang, Graff Zivin, Gross and Neidell, 2019; Ebenstein, Lavy and Roth, 2016; Greenstone et al., 2015; Bedi, Nakaguma, Restrepo and Rieger, 2021; Borgschulte, Molitor and Zou, Forthcoming; Hanna and Oliva, 2015).

4.2 Strategic Pollution Reductions and Implications for Coasian Bargaining

For water pollution, several previous studies find that a country or local government might take advantage of pollution spillovers by strategically allocating the flow of their water pollution (Sigman, 2002; Wang and Wang, 2021; He, Wang and Zhang, 2020). To our knowledge, such strategic allocation has not been investigated for air pollution, but in theory it is possible because a country or a local government is likely to have incentives to do so. If China made such a strategic decision on where to reduce air pollution during the “war on pollution,” it may have prioritized reducing air pollution for its citizens, and therefore air pollution may have decreased less for those living in neighboring countries. This strategic decision could lower the overall potential international spillover benefit.

To test this hypothesis, we use HYSPLIT to calculate the “in-China ratio” of the air pollution trajectories for each of 783 cities in China. We obtain the in-China ratio using the following approach. For each city, day, and hour, we use HYSPLIT to obtain forward trajectories of air pollution. We then compute the in-China ratio based on the number of forward trajectories that

stayed within China divided by the total number of trajectories. We consider that a pollution trajectory stayed within China if the trajectory remained inside the latitude and longitude boundaries of China or if its altitude remains below 1 km since the start of the forward trajectory.

In Figure 7, we divide Chinese cities into four groups based on the quartile of the in-China ratio. For example, cities in the first group have the lowest in-China ratio, meaning that air pollution trajectories are less likely to fall within China. We compare the declines in $PM_{2.5}$ levels relative to 2015 among the four groups. The figure suggests that the first quartile group experienced a reduction in $PM_{2.5}$ by $9.29 \mu\text{g}/\text{m}^3$, which is similar to the reduction in transboundary $PM_{2.5}$ levels for South Korea ($9.63 \mu\text{g}/\text{m}^3$). By contrast, the fourth quartile group had a $PM_{2.5}$ reduction of $18.32 \mu\text{g}/\text{m}^3$. In Tables A.11 and A.12, we show that these differences in $PM_{2.5}$ reductions between the first quartile group and other groups are statistically significant.²⁴

This result provides suggestive evidence that China may have indeed made a strategic decision on where to reduce air pollution for “the war on pollution.”²⁵ Consequently, the international spillover benefit we calculated in the previous section may have been reduced due to this strategic decision compared to a counterfactual scenario in which such a strategic decision was absent or one in which China and South Korea engaged in Coasian bargaining to address this problem.

Coase (1960) describes that one of the challenging issues of applying Coasian bargaining in practice is measuring the bargaining benefit. This is especially true for environmental externalities in international contexts. For the international spillover of air pollution from China to South Korea, our result can be used to measure the potential benefit from this bargaining. In the second row of Table 8, we consider a counterfactual scenario and calculate the potential benefits of China’s air pollution reductions. Suppose China reduced its transboundary $PM_{2.5}$ levels by $14.07 \mu\text{g}/\text{m}^3$, which was the average reduction in $PM_{2.5}$ levels in China during our sample period. In

²⁴In Table A.15, we examine whether these four groups are systematically different in other aspects but do not find systematic differences in economic variables such as GDP per capita and population.

²⁵We want to emphasize that this is suggestive evidence because the in-china ratio is not randomly assigned, and therefore, we need to rely on the standard identification assumption—given the control variables, the in-china ratio needs to be uncorrelated with the error term in the regression. One threat to this assumption is that the Chinese government might have focused on pollution reductions in cities with higher oil and coal production as these industries are major sources of air pollution, not necessarily thinking of minimizing pollution exposures to domestic residents. In Table A.12, we show that our results are robust to the inclusions of coal and oil production as additional controls.

this case, the benefit of this reduction is \$4.09 billion per year for South Korea. While there may be many other obstacles to employing Coasian bargaining in practice, the results in Table 8 provide key measurements for these countries to consider whether a certain form of agreement and compensation scheme on transboundary air pollution can be worthwhile.

5 Conclusion

In this study, we develop a framework that integrates recent advances in atmospheric science into econometric estimation with microdata on mortality and health to study the international spillover effects of air pollution. Combining transboundary particle trajectory data with the universe of individual-level mortality and emergency department visit data in South Korea, we find that transboundary air pollution from China significantly increases mortality and morbidity in South Korea. Using our estimates, we quantify that a recent Chinese environmental regulation “the war on pollution” had a substantial international spillover benefit. Our results suggest that a country’s environmental policies could generate substantial hidden benefits for neighboring countries. Finally, we demonstrate that China’s potentially strategic reductions in pollution could have undermined these benefits, highlighting the implications for additional gains through Coasian bargaining.

References

- Angrist, Joshua D., and Guido W. Imbens.** 1995. “Identification and estimation of local average treatment effects.” National Bureau of Economic Research.
- Barwick, Panle Jia, Shanjun Li, Deyu Rao, and Nahim Bin Zahur.** 2018. “The morbidity cost of air pollution: evidence from consumer spending in China.” *Available at SSRN 2999068*.
- Bedi, Arjun S, Marcos Y Nakaguma, Brandon J Restrepo, and Matthias Rieger.** 2021. “Particle pollution and cognition: Evidence from sensitive cognitive tests in Brazil.” *Journal of the Association of Environmental and Resource Economists*, 8(3): 443–474.

- Bhardwaj, Piyush, Seo J Ki, Youn H Kim, Jung H Woo, Chang K Song, Soon Y Park, and Chul H Song.** 2019. “Recent changes of trans-boundary air pollution over the Yellow Sea: implications for future air quality in South Korea.” *Environmental Pollution*, 247: 401–409.
- Borgschulte, M, D Molitor, and EY Zou.** Forthcoming. “Air pollution and the labor market: Evidence from wildfire smoke.” *Review of Economics and Statistics*.
- Burke, Marshall, Marissa L Childs, Brandon de la Cuesta, Minghao Qiu, Jessica Li, Carlos F Gould, Sam Heft-Neal, and Michael Wara.** 2023. “The contribution of wildfire to PM_{2.5} trends in the USA.” *Nature*, 622(7984): 761–766.
- Cameron, A Colin, Jonah B Gelbach, and Douglas L Miller.** 2011. “Robust inference with multiway clustering.” *Journal of Business & Economic Statistics*, 29(2): 238–249.
- Chang, Tom Y, Joshua Graff Zivin, Tal Gross, and Matthew Neidell.** 2019. “The effect of pollution on worker productivity: evidence from call center workers in China.” *American Economic Journal: Applied Economics*, 11(1): 151–72.
- Cheung, Chun Wai, Guojun He, and Yuhang Pan.** 2020. “Mitigating the air pollution effect? The remarkable decline in the pollution-mortality relationship in Hong Kong.” *Journal of environmental economics and management*, 101: 102316.
- Coase, RH.** 1960. “The Problem of Social Cost.” *The Journal of Law & Economics*, 3: 1–44.
- Deryugina, Tatyana, Garth Heutel, Nolan H Miller, David Molitor, and Julian Reif.** 2019. “The mortality and medical costs of air pollution: Evidence from changes in wind direction.” *American Economic Review*, 109(12): 4178–4219.
- Deschênes, Olivier, and Enrico Moretti.** 2009. “Extreme weather events, mortality, and migration.” *The Review of Economics and Statistics*, 91(4): 659–681.

- Ebenstein, Avraham, Victor Lavy, and Sefi Roth.** 2016. “The long-run economic consequences of high-stakes examinations: Evidence from transitory variation in pollution.” *American Economic Journal: Applied Economics*, 8(4): 36–65.
- Eguiluz-Gracia, Ibon, Alexander G Mathioudakis, Sabine Bartel, Susanne JH Vijverberg, Elaine Fuertes, Pasquale Comberiati, Yutong Samuel Cai, Peter Valentin Tomazic, Zuzana Diamant, Jørgen Vestbo, et al..** 2020. “The need for clean air: the way air pollution and climate change affect allergic rhinitis and asthma.” *Allergy*, 75(9): 2170–2184.
- Fowlie, Meredith, Edward A Rubin, and Katie Wright.** 2021. “Air Pollution Co-Benefits and Regulatory Rebound.” *Presentation at UC Berkeley Energy Camp*.
- Greenstone, Michael, Guojun He, Shanjun Li, and Eric Yongchen Zou.** 2021. “China’s war on pollution: Evidence from the first 5 years.” *Review of Environmental Economics and Policy*, 15(2): 281–299.
- Greenstone, Michael, Janhavi Nilekani, Rohini Pande, Nicholas Ryan, Anant Sudarshan, and Anish Sugathan.** 2015. “Lower pollution, longer lives: life expectancy gains if India reduced particulate matter pollution.” *Economic and Political Weekly*, 40–46.
- Hanna, Rema, and Paulina Oliva.** 2015. “The effect of pollution on labor supply: Evidence from a natural experiment in Mexico City.” *Journal of Public Economics*, 122: 68–79.
- Han, Xiao, Juzhen Cai, Meigen Zhang, and Xiaofei Wang.** 2021. “Numerical simulation of interannual variation in transboundary contributions from Chinese emissions to PM_{2.5} mass burden in South Korea.” *Atmospheric Environment*, 256: 118440.
- He, Guojun, Shaoda Wang, and Bing Zhang.** 2020. “Watering down environmental regulation in China.” *The Quarterly Journal of Economics*, 135(4): 2135–2185.

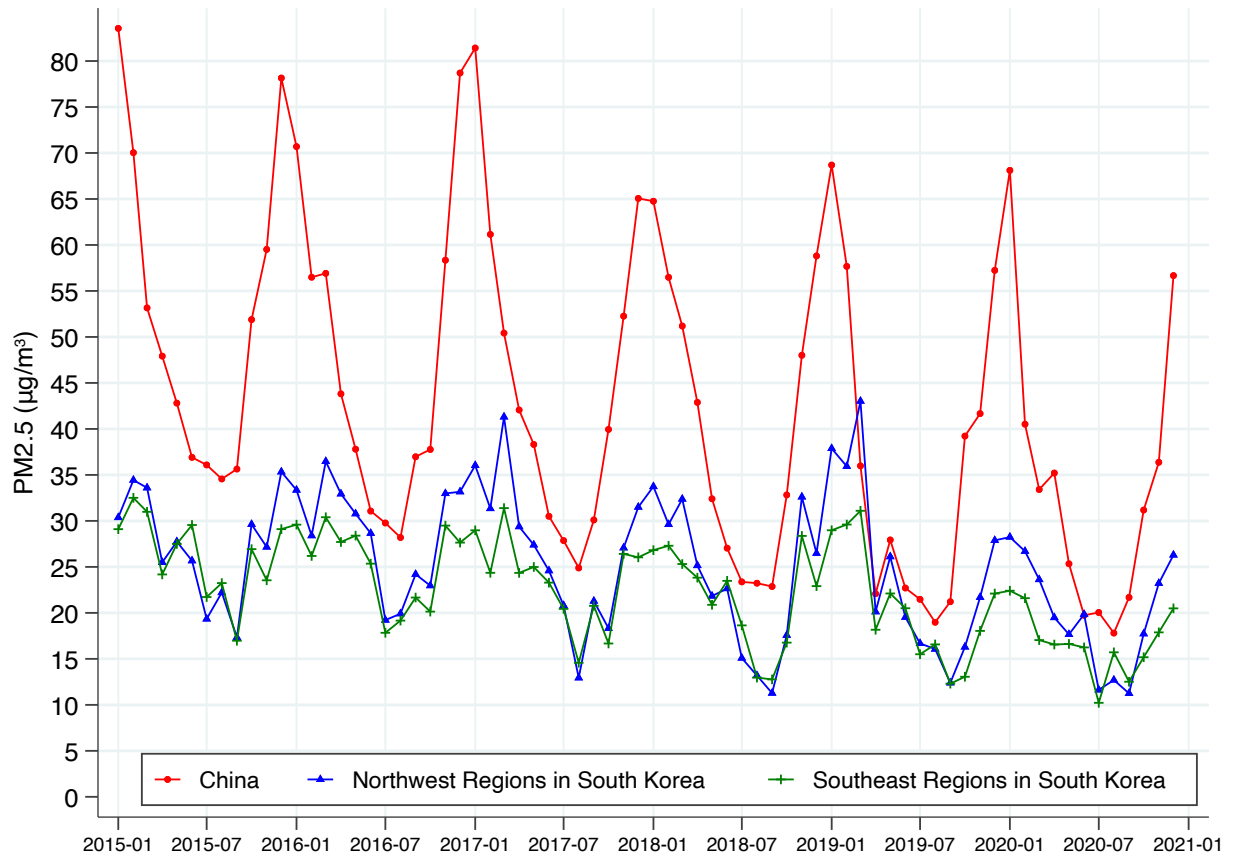
- Hernandez-Cortes, Danae, and Kyle C Meng.** 2023. “Do environmental markets cause environmental injustice? Evidence from California’s carbon market.” *Journal of Public Economics*, 217: 104786.
- Hsiang, Solomon, Jaecheol Lee, and Andrew Wilson.** 2022. “Simultaneous Estimation of Damage from Transboundary and Domestic Air Pollution.” *Presentation at the Coase Project Conference*.
- Ito, Koichiro, and Shuang Zhang.** 2020. “Willingness to Pay for Clean Air: Evidence from Air Purifier Markets in China.” *Journal of Political Economy*, 128(5): 1627–1672.
- Jia, Ruixue, and Hyejin Ku.** 2019. “Is China’s pollution the culprit for the choking of South Korea? Evidence from the Asian dust.” *The Economic Journal*, 129(624): 3154–3188.
- Kim, So Young, Seok-Jun Yoon, Min-Woo Jo, Eun-Jung Kim, Hyun-Jin Kim, and In-Hwan Oh.** 2010. “Economic burden of allergic rhinitis in Korea.” *American journal of rhinology & allergy*, 24(5): e110–e113.
- Kim, Ye-Shin, Yong-Jin Lee, Hoa-Sung Park, and Dong-Chun Shin.** 2003. “Risk-Based Damage Cost Estimation on Mortality Due to Environmental Problems.” *Journal of Preventive Medicine and Public Health*, 36(3): 230–238. Publisher: The Korean Society for Preventive Medicine.
- Kuiper, Ingrid Nordeide, Cecilie Svanes, Iana Markevych, Simone Accordini, Randi J Bertelsen, Lennart Bråbäck, Jesper Heile Christensen, Bertil Forsberg, Thomas Halvorsen, Joachim Heinrich, et al..** 2021. “Lifelong exposure to air pollution and greenness in relation to asthma, rhinitis and lung function in adulthood.” *Environment international*, 146: 106219.
- Lee, Hyung-Min, Rokjin J Park, Daven K Henze, Seungun Lee, Changsub Shim, Hye-Jung Shin, Kwang-Joo Moon, and Jung-Hun Woo.** 2017a. “PM2. 5 source attribution for Seoul in May from 2009 to 2013 using GEOS-Chem and its adjoint model.” *Environmental Pollution*, 221: 377–384.

- Lee, Seungmin, Chang-Hoi Ho, Yun Gon Lee, Hyoung-Jin Choi, and Chang-Keun Song.** 2013. “Influence of transboundary air pollutants from China on the high-PM10 episode in Seoul, Korea for the period October 16–20, 2008.” *Atmospheric Environment*, 77: 430–439.
- Lee, Yong Jin, Young Wook Lim, Ji Yeon Yang, Chang Soo Kim, Young Chul Shin, and Dong Chun Shin.** 2011. “Evaluating the PM damage cost due to urban air pollution and vehicle emissions in Seoul, Korea.” *Journal of Environmental Management*, 92(3): 603–609.
- Lee, Yoo Ju, Sun-Hong Kwon, Sung-Hyun Hong, Jin Hyun Nam, Hyun Jin Song, Jong Seop Lee, Eui-Kyung Lee, and Ju-Young Shin.** 2017*b*. “Health care utilization and direct costs in mild, moderate, and severe adult asthma: a descriptive study using the 2014 South Korean Health Insurance Database.” *Clinical therapeutics*, 39(3): 527–536.
- MicroData Integrated Service.** 1997–2019. “Causes of Death Statistics (Public Use).” <https://doi.org/10.23333/P.101054.001>. (Accessed March 23, 2022).
- Monogan III, James E, David M Konisky, and Neal D Woods.** 2017. “Gone with the wind: Federalism and the strategic location of air polluters.” *American Journal of Political Science*, 61(2): 257–270.
- Morehouse, John, and Edward Rubin.** 2021. “Downwind and out: The strategic dispersion of power plants and their pollution.” *Available at SSRN 3915247*.
- Murphy, Kevin M, and Robert H Topel.** 2006. “The value of health and longevity.” *Journal of Political Economy*, 114(5): 871–904.
- National Health Insurance Sharing Service.** 2013–2017. “Environmental Illness Database.” (Accessed August 30, 2021).
- Oh, Hye-Ryun, Chang-Hoi Ho, Jinwon Kim, Deliang Chen, Seungmin Lee, Yong-Sang Choi, Lim-Seok Chang, and Chang-Keun Song.** 2015. “Long-range transport of air pollutants orig-

- inating in China: A possible major cause of multi-day high-PM10 episodes during cold season in Seoul, Korea.” *Atmospheric Environment*, 109: 23–30.
- Rohde, Robert A, and Richard A Muller.** 2015. “Air pollution in China: mapping of concentrations and sources.” *PloS one*, 10(8): e0135749.
- Ryan, Anna C, Deonie Allen, Steve Allen, Vittorio Maselli, Amber LeBlanc, Liam Kelleher, Stefan Krause, Tony R Walker, and Mark Cohen.** 2023. “Transport and deposition of ocean-sourced microplastic particles by a North Atlantic hurricane.” *Communications Earth & Environment*, 4(1): 442.
- Sheldon, Tamara L, and Chandini Sankaran.** 2017. “The impact of Indonesian forest fires on Singaporean pollution and health.” *American Economic Review*, 107(5): 526–29.
- Shin, Young Chul, and Seunghun Joh.** 2003. “Estimating the Willingness-to-Pay and the Value of a Statistical Life for Future Mortality Risk Reduction : The Value of a Statistical Life for Assessing Environmental Damages and Policies.” *Environmental and Resource Economics Review*, 12(1): 49–74. Publisher: Korean Resource Economics Association.
- Sigman, Hilary.** 2002. “International spillovers and water quality in rivers: do countries free ride?” *American Economic Review*, 92(4): 1152–1159.
- Stein, AF, Roland R Draxler, Glenn D Rolph, Barbara JB Stunder, MD Cohen, and Fong Ngan.** 2015. “NOAA’s HYSPLIT atmospheric transport and dispersion modeling system.” *Bulletin of the American Meteorological Society*, 96(12): 2059–2077.
- Wang, Shaoda, and Zenan Wang.** 2021. “The environmental and economic consequences of internalizing border spillovers.”
- World Bank.** 2022. *Striving for Clean Air: Air Pollution and Public Health in South Asia*. Washington, D.C.:World Bank Group. <http://documents.worldbank.org/curated/en/099030312132233780/P1682370b4ac4a0270ac2702e1cfb704198>.

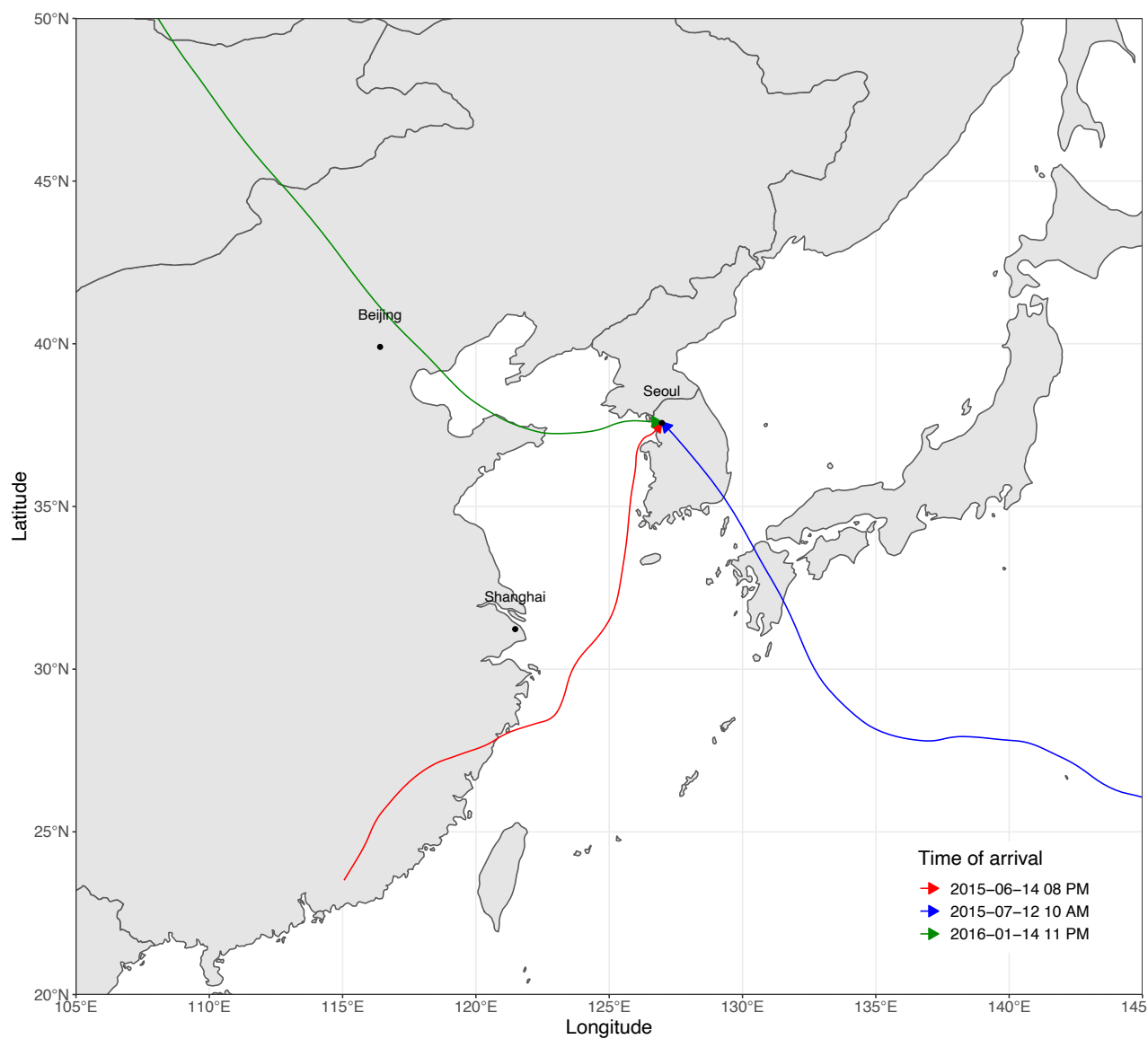
Figures

Figure 1: PM_{2.5} in China and South Korea



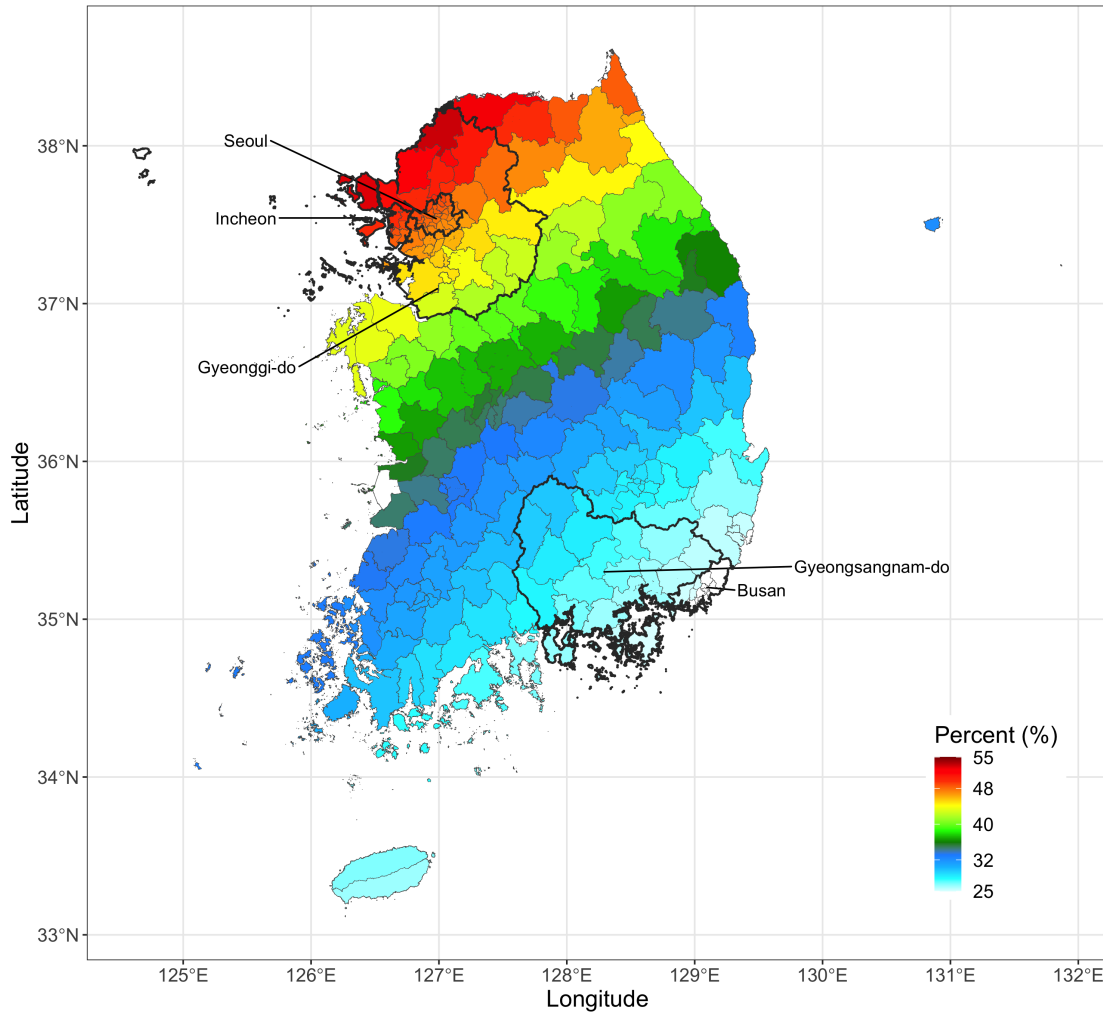
Note: This figure illustrates the evolution of monthly average levels of hourly PM_{2.5} concentration. The Northwest region in South Korea is defined as cities in South Korea with at least 35% of trajectories coming from China (see Figure 3). The Southwest region in South Korea is defined as cities with less than 35% of trajectories coming from China.

Figure 2: Examples of Backward Trajectories



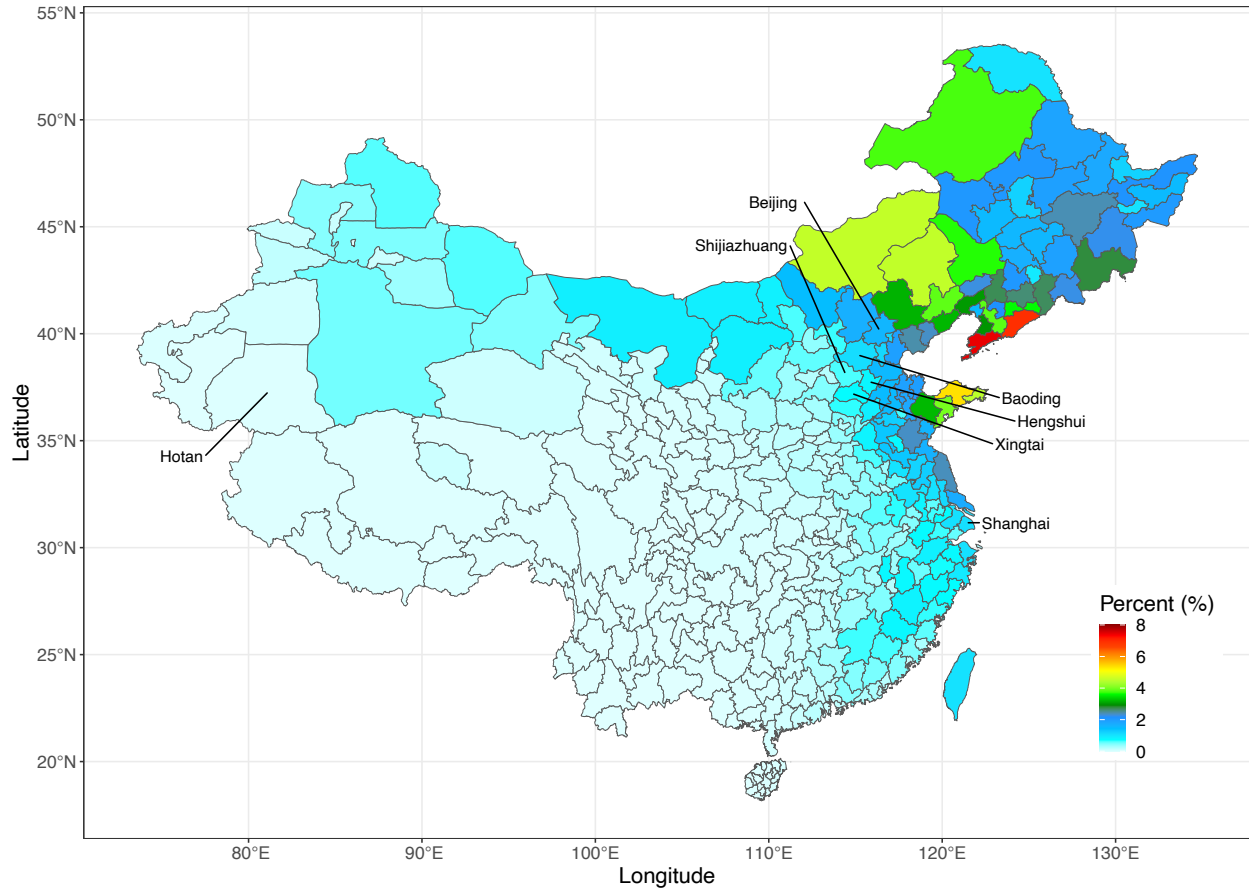
Note: This figure shows three examples of backward trajectories obtained from HYSPLIT. For example, the green trajectory came from northern China, passed through Beijing, and reached Seoul at 11 pm on January 14, 2016.

Figure 3: Frequency of Trajectories Coming from China



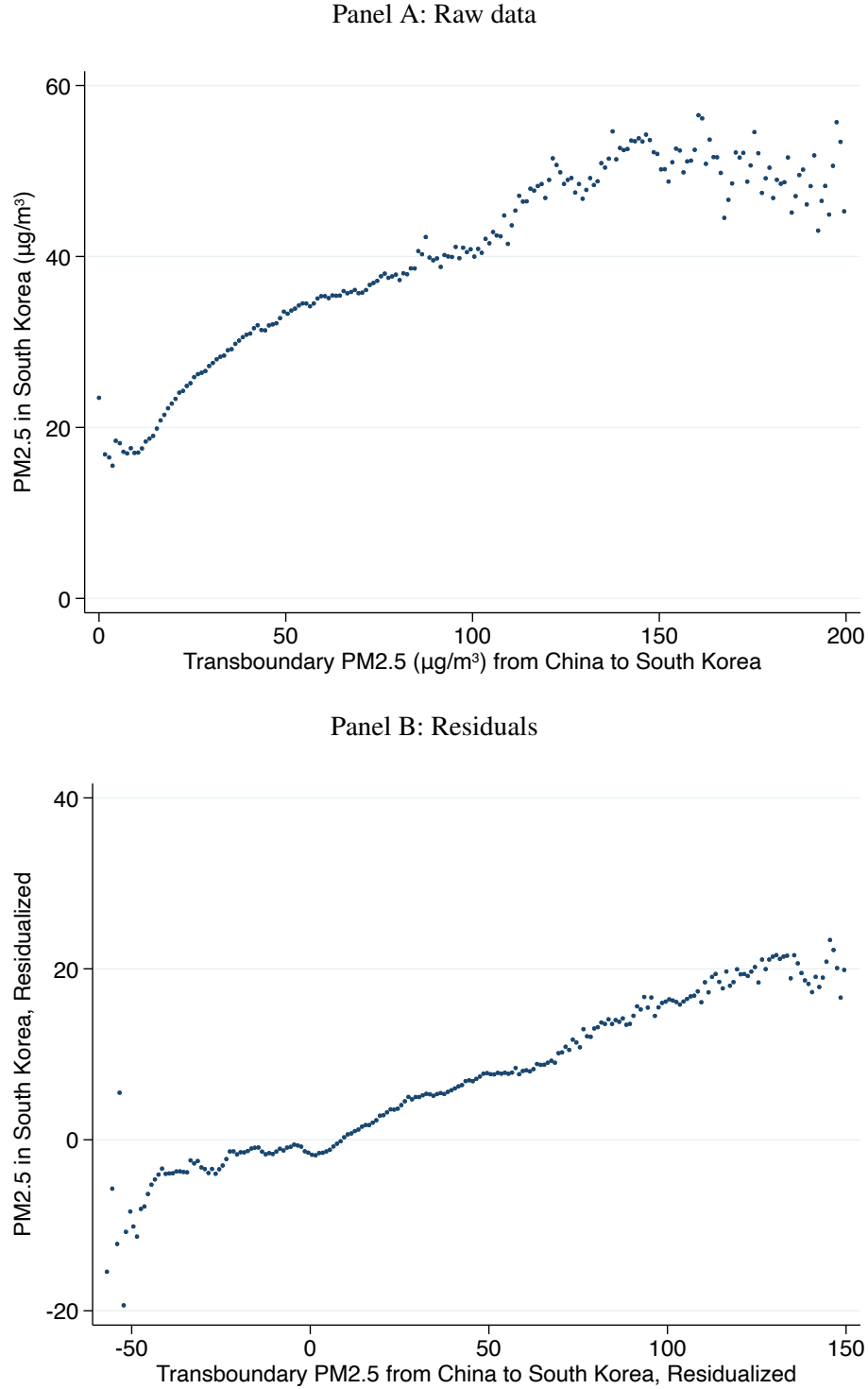
Note: This figure shows the percentage of hours in which each city in South Korea had trajectories coming from China during our sample period (January 2015 to December 2019). For each city in South Korea, we use the HYSPLIT model to obtain backward trajectories for each day-hour. We then compute the percentage of backward trajectories that came from China. That is, the denominator is the total number of hours from January 1, 2015 to December 31, 2019, and the numerator is the total number of hours in which the trajectories came from China. The duration of the backward trajectories we use is 200 hours. For example, if this value is 50% for a city in South Korea, it means that in half of the total hours in our sample period, this city had the trajectories coming from China.

Figure 4: Frequencies of Trajectories From China to South Korea



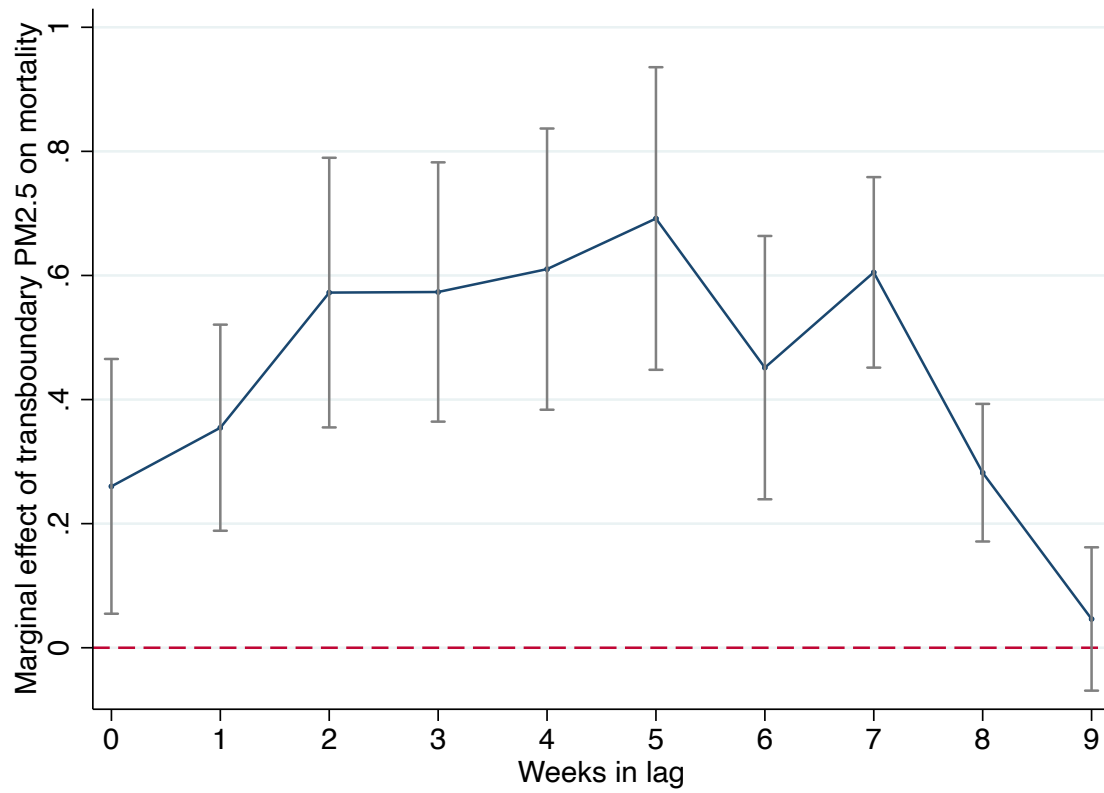
Note: This figure shows how often each city in China had a trajectory that passed the city and reached South Korea. For each city in South Korea, we use the HYSPLIT model to obtain backward trajectories for each day-hour during our sample period (January 2015 to December 2019). We then compute how often these backward trajectories passed each city in China. That is, the denominator is the total number of hours from January 1, 2015 to December 31, 2019. The numerator is the total number of hours in which a trajectory passed a city in China and reached cities in South Korea. For example, if this value is 5% for a city in China, it means that in 5% of the total hours in our sample period, a trajectory passed this city and reached a city in South Korea. The duration of the backward trajectories we use is 200 hours (we find that more than 99% of the trajectories that come from China to South Korea have duration less than 200 hours, as shown in Figure A.5).

Figure 5: Scatter Plot of $PM_{2.5}$ in South Korea and Transboundary $PM_{2.5}$ from China



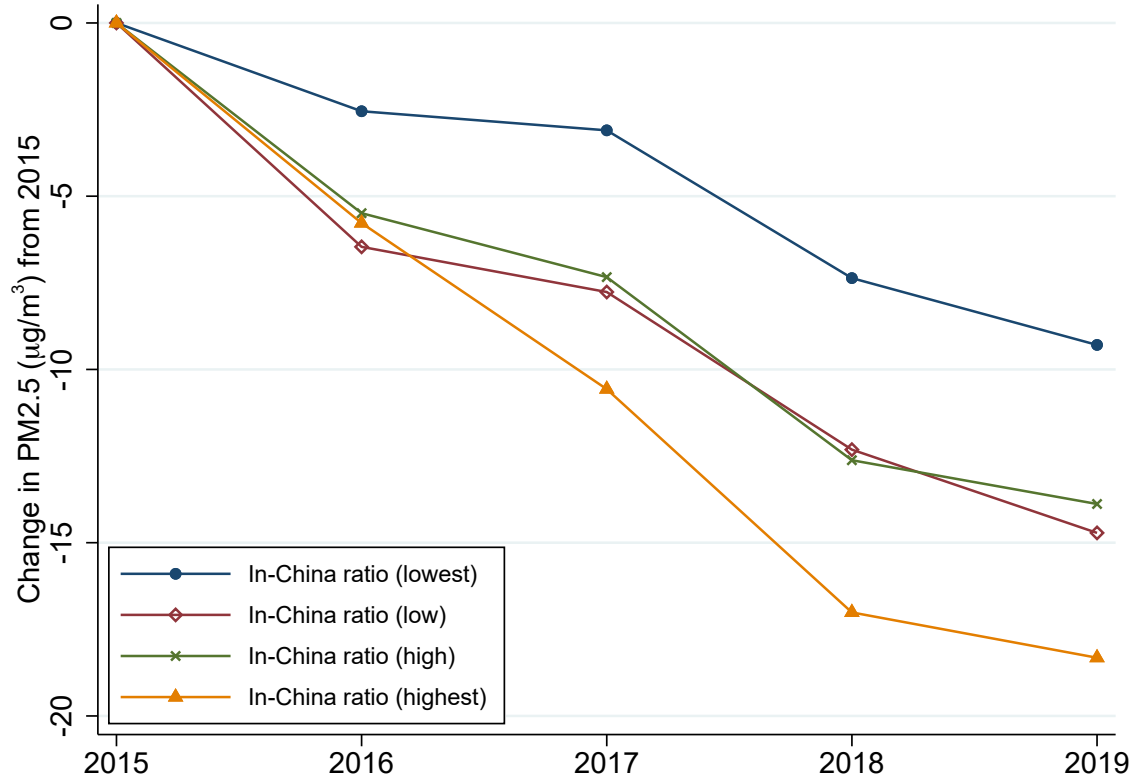
Note: Panel A plots the mean of $PM_{2.5}$ levels within each bin against the mean of transboundary $PM_{2.5}$ levels within each bin (with bins of size $1 \mu g/m^3$). Panel B plots the mean of residuals (from a regression of $PM_{2.5}$ levels in South Korea on city-by-year-by-month fixed effects, city-by-day of week fixed effects, city-by-rainfall quartile fixed effects, and city-by-temperature quartile fixed effects) against bins of residuals (from a regression of transboundary $PM_{2.5}$ on city-by-year-by-month fixed effects, city-by-day of week fixed effects, city-by-rainfall quartile fixed effects, and city-by-temperature quartile fixed effects).

Figure 6: Weekly Lagged Effects of Transboundary Air Pollution on Mortality



Note: This figure plots the estimates and 95% confidence intervals presented in Panel B of Table 3. Each point estimate indicates the partial lagged marginal effect of transboundary PM_{2.5} (traveling from China to Korea) on hourly mortality per billion people in South Korea.

Figure 7: Testing for Strategic Air Pollution Reductions in China



Note: This figure plots the change in $PM_{2.5}$ levels relative to the 2015 level for Chinese cities, grouped by quartiles of the in-China ratio. The in-China ratio is calculated by the following approach. For each city, day, and hour, we use HYSPLIT to obtain forward air pollution trajectories. We then compute the in-China ratio based on the number of trajectories that entered China divided by the total number of trajectories. A pollution trajectory is considered to have fallen within China if the trajectory falls inside the latitude and longitude boundaries of China or if the trajectory's altitude is persistently below 1 km since the start of the forward trajectory. We provide the statistical analysis of this relationship with a set of control variables in Tables A.11 and A.12.

Tables

Table 1: Summary Statistics

	Mean	Standard Deviation	Number of Observations
<i>A. Data at the city-by-hour level</i>			
PM _{2.5} in Chinese cities (µg/m ³)	45.05	38.40	30,844,642
PM _{2.5} in South Korean cities (µg/m ³)	24.99	18.06	9,585,947
Transboundary PM _{2.5} from China to Korean cities (µg/m ³)	14.49	26.34	9,741,674
Mortality rates in South Korea (hourly deaths per billion people)			
Overall	894	3,800	9,991,872
Respiratory/Cardiovascular	231	1,954	9,991,872
Infant (age < 1)	327	27,702	9,991,872
Elderly (age ≥ 65)	3,576	14,197	9,991,872
Hourly Temperature (°C)	13.01	10.43	9,966,769
Hourly Precipitation (mm)	0.13	1.00	9,942,103
<i>B. Data at the city-by-day level</i>			
Emergency room visits (counts per billion people)			
Atopic	0.08	0.32	250,116
Rhinitis	3.27	5.68	250,116
Asthma	2.15	2.65	250,116
<i>C. Data at the city-by-year level</i>			
Population (in thousands)			
Overall	232.35	240.08	1,140
Elderly (age ≥ 65)	32.52	25.58	1,140
Infant (age < 1)	1.63	1.86	1,140

Note: This table reports summary statistics. All PM_{2.5} levels are in micrograms per cubic meter of air, abbreviated as µg/m³. All mortality rates are hourly deaths per billion people in the corresponding age group. The sample includes all South Korean cities and 784 Chinese cities over a period of January 2015 to December 2019.

Table 2: First Stage: Impacts of Transboundary Air Pollution on Local Air Quality in South Korea

Dependent variable: Hourly PM _{2.5} levels in South Korean cities				
	(1)	(2)	(3)	(4)
Hourly Transboundary PM _{2.5}	0.180 (0.003)	0.137 (0.002)	0.137 (0.002)	0.137 (0.002)
Constant	22.551 (0.327)			
Observations	9,342,033	9,287,734	9,287,734	9,287,734
KP F-stat	2,884	3,647	3,945	3,953
Year-Month-City FE	No	No	Yes	Yes
Year-Month FE	No	Yes	No	No
Month-City FE	No	Yes	No	No
Month-Province FE	No	No	No	No
City FE	Yes	Yes	Yes	Yes
Day of week-City FE	No	Yes	Yes	Yes
Rainfall quartile-City FE	No	Yes	No	Yes
Temperature quartile-City FE	No	Yes	No	Yes
Rainfall quartile FE	No	No	Yes	No
Temperature quartile FE	No	No	Yes	No

Note: This table shows OLS estimation results for equation (1). Two-way cluster-robust standard errors at the city and hour levels are reported in parentheses. All models are weighted by the city population. The KP F-stat is the Kleibergen-Paap rk Wald F statistic. The sample includes all South Korean cities between January 2015 and December 2019.

Table 3: Impacts of Transboundary Air Pollution on Mortality in South Korea (Reduced-form)

Panel A: Average Effect Over Past 70 Days (Dependent variable: hourly mortality per billion people)				
	Overall	Elderly	Infant	Respiratory/ cardiovascular
Transboundary PM _{2.5} (past 0-70 days)	3.60 (0.63)	19.09 (4.20)	6.93 (2.78)	1.67 (0.23)
Observations	9,555,368	9,555,368	9,555,368	9,555,368
Mean of dependent variable	618	3,259	314	148
Marginal effect on mortality (%)	0.6%	0.6%	2.2%	1.1%
Marginal effect on annual mortality/million	31.6	167.3	60.7	14.7
Panel B: Weekly Lagged Effects (Dependent variable: hourly mortality per billion people)				
	Overall	Elderly	Infant	Respiratory/ cardiovascular
Transboundary PM _{2.5} (past 0-7 days)	0.26 (0.10)	1.30 (0.68)	0.79 (0.57)	0.13 (0.04)
Transboundary PM _{2.5} (past 7-14 days)	0.35 (0.08)	2.03 (0.57)	0.43 (0.66)	0.21 (0.03)
Transboundary PM _{2.5} (past 14-21 days)	0.57 (0.11)	3.30 (0.70)	1.71 (0.60)	0.27 (0.05)
Transboundary PM _{2.5} (past 21-28 days)	0.57 (0.11)	3.51 (0.65)	0.03 (0.47)	0.26 (0.04)
Transboundary PM _{2.5} (past 28-35 days)	0.61 (0.12)	3.45 (0.79)	1.33 (0.69)	0.24 (0.05)
Transboundary PM _{2.5} (past 35-42 days)	0.69 (0.12)	4.08 (0.69)	0.27 (0.77)	0.32 (0.05)
Transboundary PM _{2.5} (past 42-49 days)	0.45 (0.11)	2.27 (0.66)	1.27 (0.73)	0.16 (0.05)
Transboundary PM _{2.5} (past 49-56 days)	0.60 (0.08)	3.53 (0.57)	0.90 (0.71)	0.23 (0.03)
Transboundary PM _{2.5} (past 56-63 days)	0.28 (0.06)	1.63 (0.42)	0.48 (0.49)	0.11 (0.02)
Transboundary PM _{2.5} (past 63-70 days)	0.05 (0.06)	-0.40 (0.41)	0.92 (0.73)	0.06 (0.02)
Observations	9,555,368	9,555,368	9,555,368	9,555,368
Mean of dependent variable	618	3,259	314	148

Note: This table shows OLS estimation results for equation (2). Two-way cluster-robust standard errors at the city and hour levels are reported in parentheses. All regressions include city-by-year-by-month fixed effects, city-by-day of week fixed effects, city-by-rainfall quartile fixed effects, city-by-temperature quartile fixed effects, and are weighted by city-level population. The sample includes all South Korean cities between January 2015 and December 2019.

Table 4: Impacts of Local Air Quality on Mortality in South Korean Cities (IV Estimation)

Panel A: Average Effect Over the Past 70 Days (Dependent variable: hourly mortality per billion people)

	Overall	Elderly	Infant	Respiratory/ cardiovascular
PM _{2.5} (past 0-70 days)	9.26 (1.65)	49.07 (10.82)	18.22 (7.33)	4.30 (0.60)
Observations	9,528,960	9,528,960	9,528,960	9,528,960
Mean of dependent variable	618	3,258	314	148
Marginal effect on mortality (%)	1.5%	1.5%	5.8%	2.9%
Marginal effect on annual mortality/million	81.1	429.9	159.6	37.7

Panel B: Weekly Lagged Effects (Dependent variable: hourly mortality per billion people)

	Overall	Elderly	Infant	Respiratory/ cardiovascular
PM _{2.5} (past 0-7 days)	0.55 (0.29)	2.67 (1.89)	1.58 (1.48)	0.29 (0.10)
PM _{2.5} (past 7-14 days)	0.73 (0.23)	3.92 (1.41)	0.76 (1.84)	0.51 (0.10)
PM _{2.5} (past 14-21 days)	1.40 (0.35)	8.28 (2.20)	3.98 (2.03)	0.73 (0.15)
PM _{2.5} (past 21-28 days)	1.33 (0.30)	8.13 (1.89)	-0.33 (1.82)	0.70 (0.12)
PM _{2.5} (past 28-35 days)	1.33 (0.28)	7.59 (2.00)	3.72 (1.64)	0.54 (0.11)
PM _{2.5} (past 35-42 days)	1.85 (0.32)	11.36 (1.78)	0.67 (2.07)	0.81 (0.14)
PM _{2.5} (past 42-49 days)	1.55 (0.35)	8.28 (2.25)	3.58 (2.06)	0.56 (0.16)
PM _{2.5} (past 49-56 days)	2.36 (0.30)	13.98 (1.92)	3.78 (2.50)	0.86 (0.13)
PM _{2.5} (past 56-63 days)	1.46 (0.23)	9.15 (1.45)	1.57 (1.35)	0.52 (0.11)
PM _{2.5} (past 63-70 days)	0.05 (0.15)	-1.41 (1.05)	2.54 (1.88)	0.08 (0.06)
Observations	9,274,113	9,274,113	9,274,113	9,274,113
Mean of dependent variable	617	3,260	315	148

Note: This table shows instrumental variable estimation results for equation (3). Two-way cluster-robust standard errors at the city and hour levels are reported in parentheses. All columns include city-by-year-by-month fixed effects, city-by-day of week fixed effects, city-by-rainfall quartile fixed effects, city-by-temperature quartile fixed effects, and are weighted by city-level population. The Kleibergen-Paap rk Wald F statistic is 1,478 for all columns in Panel A and 221 for all columns in Panel B.

Table 5: Impacts of Transboundary Air Pollution on Mortality by Age Group

Panel A: Reduced Form (Dependent variable: hourly mortality per billion people)						
	Infant	1-9	10-19	20-29	30-39	40-49
Transboundary PM _{2.5} (past 0-70 days)	6.94 (2.78)	0.19 (0.21)	-0.24 (0.18)	0.15 (0.18)	0.99 (0.38)	0.58 (0.32)
Mean of dependent variable	314	12	18	42	79	169
Marginal effect as % increase in mortality	2.2%	1.5%	-1.3%	0.4%	1.3%	0.3%
Marginal effect on annual mortality/million	60.8	1.7	-2.1	1.4	8.7	5.1
	50-59	60-69	70-79	80-89	90-99	100-109
Transboundary PM _{2.5} (past 0-70 days)	3.08 (0.62)	4.47 (1.15)	13.18 (4.20)	41.63 (10.71)	104.54 (45.33)	231.28 (167.79)
Mean of dependent variable	364	746	2,313	7,324	19,368	16,318
Marginal effect as % increase in mortality	0.8%	0.6%	0.6%	0.6%	0.5%	1.4%
Marginal effect on annual mortality/million	27.0	39.1	115.4	364.6	915.7	2026.1
Panel B: IV Estimation (Dependent variable: hourly mortality per billion people)						
	Infant	1-9	10-19	20-29	30-39	40-49
PM _{2.5} (past 0-70 days)	18.22 (7.33)	0.48 (0.55)	-0.59 (0.48)	0.40 (0.47)	2.58 (1.00)	1.54 (0.83)
Mean of dependent variable	314	12	18	42	79	169
Marginal effect as % increase in mortality	5.8%	3.8%	-3.3%	1.0%	3.3%	0.9%
Marginal effect on annual mortality/million	159.6	4.2	-5.2	3.5	22.6	13.5
	50-59	60-69	70-79	80-89	90-99	100-109
PM _{2.5} (past 0-70 days)	7.98 (1.73)	11.36 (3.01)	33.48 (10.90)	107.65 (27.96)	270.80 (116.58)	591.13 (429.42)
Mean of dependent variable	364	746	2,312	7,322	19,365	16,323
Marginal effect as % increase in mortality	2.2%	1.5%	1.4%	1.5%	1.4%	3.6%
Marginal effect on annual mortality/million	69.9	99.5	293.3	943.0	2372.2	5178.3

Note: Panel A shows age-specific results for the OLS estimation in equation (2), and Panel B shows results for the instrumental variable estimation in equation (3). Two-way cluster-robust standard errors at the city and hour levels are reported in parentheses. In the OLS estimation, all age groups have 9,555,368 observations, except for the age group 100-109, which has 9,537,950 observations. The age group 100-109 has fewer observations because the population for age over 100 is 0 for some years in some cities in the sample. In the IV estimation, all age groups have 9,528,950 observations, except for the age group 100-109, which has 9,511,542 observations. All regressions include city-by-year-by-month fixed effects, city-by-day of week fixed effects, city-by-rainfall quartile fixed effects, city-by-temperature quartile fixed effects, and are weighted by city-level population. The Kleibergen-Paap rk Wald F statistic for Panel B is 1,478 for all age groups except for age group 100-109 (1,475). The sample includes all South Korean cities between January 2015 and December 2019.

Table 6: The Impact of Transboundary Air Pollution on Emergency Department Visits

Panel A: Reduced-form Estimation			
	Asthma	Rhinitis	Atopic
Transboundary PM _{2.5} (past 0-60 days)	45.2 (11.1)	502.7 (56.5)	-2.3 (1.5)
Observations	234,389	234,389	234,389
Mean of dependent variable	9214.0	14037.6	364.0
Marginal effect as % increase in ED visits	0.5%	3.6%	-0.6%
Marginal effect on annual ED visits/million	16.5	183.5	-0.8

Panel B: Instrumental Variable Estimation			
	Asthma	Rhinitis	Atopic
PM _{2.5} (past 0-60 days)	181.7 (46.3)	2020.1 (254.3)	-9.2 (6.1)
Observations	234,389	234,389	234,389
Mean of dependent variable	9214.0	14037.6	364.0
Marginal effect as % increase in ED visits	2.0%	14.4%	-2.5%
Marginal effect on annual ED visits/million	66.3	737.3	-3.4

Note: Standard errors, clustered by city, are reported in parentheses. All regressions include city-by-year-by-month fixed effects, city-by-day of week fixed effects, city-by-rainfall quartile fixed effects, city-by-temperature quartile fixed effects, city-by-humidity quartile fixed effects, and are weighted by city-level population. The Kleibergen-Paap rk Wald F statistic is 637 for all columns in the IV estimation. The sample includes all South Korean cities between January 2015 and December 2017. The dependent variables are the numbers of daily ED visits per billion people due to asthma, rhinitis, and atopic dermatitis, respectively. All columns in this table include controls for pollen variables (oak, pine and weed pollen).

Table 7: The Impact of Transboundary Air Pollution and Air Pollution Alerts on Mortality

Panel A: Reduced Form (Dependent variable: hourly mortality per billion people)				
	Overall	Elderly	Infant	Respiratory/ cardiovascular
Transboundary PM _{2.5} (past 0-70 days)	4.48 (0.68)	25.31 (4.56)	4.70 (3.01)	2.01 (0.27)
Alert (past 0-70 days)	-99.84 (85.11)	-1008.15 (558.78)	613.96 (596.97)	-112.30 (35.20)
Trans. PM _{2.5} (past 0-70 days) \times Alert (past 0-70 days)	-21.22 (4.95)	-131.68 (39.17)	30.89 (41.73)	-3.47 (3.27)
Mean of dependent variable	618	3,259	314	148

Panel B: IV Estimation (Dependent variable: hourly mortality per billion people)				
	Overall	Elderly	Infant	Respiratory/ cardiovascular
PM _{2.5} (past 0-70 days)	16.20 (2.72)	90.27 (18.44)	23.80 (13.21)	7.97 (1.11)
Alert (past 0-70 days)	-946.51 (278.47)	-5408.95 (2063.96)	-2079.12 (2056.08)	-690.35 (144.77)
PM _{2.5} (past 0-70 days) \times Alert (past 0-70 days)	-30.61 (11.10)	-199.75 (88.51)	87.44 (94.63)	-0.08 (7.37)
Mean of dependent variable	618	3,258	314	148

Note: All regressions include city-by-year-by-month fixed effects, city-by-day of week fixed effects, city-by-rainfall quartile fixed effects, city-by-temperature quartile fixed effects, and are weighted by city-level population. Two-way cluster-robust standard errors at the city and hour levels are reported in parentheses. The Kleibergen-Paap rk Wald F statistic for Panel B is 806. All groups have 9,528,960 observations. The sample includes all South Korean cities between January 2015 and December 2019.

Table 8: International Spillover Benefits of Reductions in Air Pollution (\$ billion/year)

	Overall	Infant < 1	Youth 1 – 19	Adult 20 – 64	Elderly ≥ 65
Status Quo:					
Reduction of Transboundary PM _{2.5} by 9.63 µg/ m ³	2.80	0.11	0.03	1.65	1.00
Counterfactual Scenario:					
Reduction of Transboundary PM _{2.5} by 14.07 µg/ m ³	4.09	0.17	0.05	2.41	1.46

Note: This table shows the international spillover benefits of reductions in air pollution for three scenarios. The table reports the per-year spillover benefit for South Korea in 2019 US billion dollars. We calculate the benefits based on the estimates of the age-specific impacts of transboundary air pollution on mortality in Table and the age-specific value of a statistical life described in Section 4. The status quo is based on the actual reduction in transboundary air pollution from China to South Korea observed in our data during our sample period (9.63 µg/m³). The counterfactual scenario is based on the national-average pollution reduction in China during our sample period (14.07 µg/m³).

Appendix A Details of the HYSPLIT model

In this section, we provide details of the Hybrid Single-Particle Lagrangian Integrated Trajectory model (HYSPLIT), an open-source computer software for simulating atmospheric transport and dispersion.²⁶

Brief description of the HYSPLIT model

Developed by the National Oceanic and Atmospheric Administration (NOAA) Air Resources Laboratory and the Australian Bureau of Meteorology Research Centre in 1998, HYSPLIT computes trajectories of particles to determine how far and where particles will travel. The model can also simulate particle dispersion and compute air concentrations. However, we focus our attention on trajectory computation, because our study is concerned with determining whether pollutants in South Korea passed through China. Particle dispersion is useful when estimating the effect of emissions from point sources, such as factories and power plants.

To compute a forward trajectory or a backward trajectory, the model takes a coordinate and a height of a starting location, a starting time, a trajectory duration, and other parameters as inputs and computes a trajectory of a single particle using the mean wind speed and direction of each grid that the particle passes by.²⁷ The forward trajectory is calculated by tracking the movement of the air mass in time, whereas the backward trajectory is calculated by tracking the movement of the air mass *back* in time. Forward trajectory analysis is useful for determining the particle dispersion, while backward trajectory analysis is useful for determining the origins of pollutants.

Figure A.1 shows how forward trajectories are calculated in the HYSPLIT model. Given the initial position $P(t)$ and the first-guess position $P'(t + \Delta t) = P(t) + V(P, t)\Delta t$ where $V(P, t)$ denote the velocity vector, $V(P, t)$ is linearly interpolated, which is then used to obtain the final position:

$$P(t + \Delta t) = P(t) + \frac{V(P, t) + V(P', t + \Delta t)}{2} \cdot \Delta t.$$

Backward trajectories are calculated using the same procedure, except that Δt is now negative.

Comparison between different methods of analysis in the HYSPLIT model

The purpose of using the HYSPLIT model is to determine whether pollution in South Korea at a given time comes from China. To address this question, we explored a number of possible options using the HYSPLIT model.

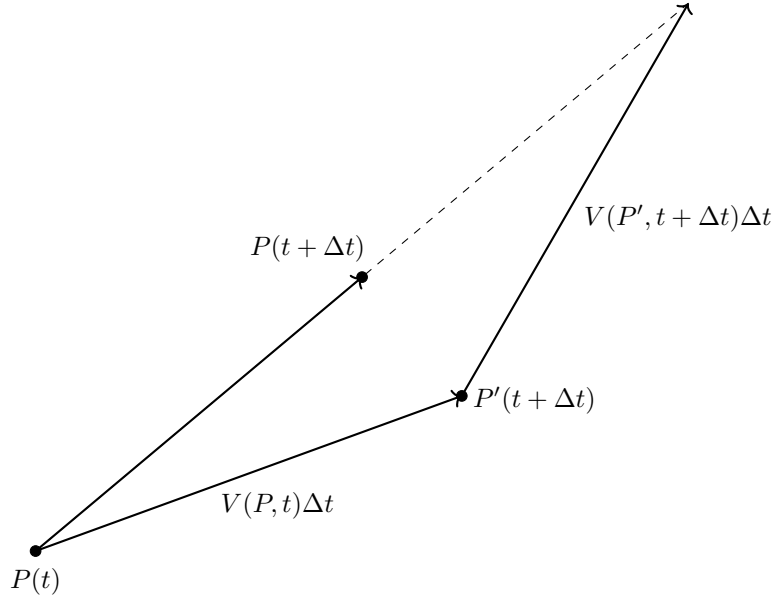
First, we discuss the benefits and limitations of forward and backward trajectory analyses. Forward trajectory analysis is useful for determining emission paths or dispersion of pollutants from a point source. For example, [Hernandez-Cortes and Meng \(2023\)](#) computes concentrations of air pollutants for each zip code and year by running forward trajectory simulations from each facility in California. To address our research question, one may imagine running forward trajectory simulations from polluting facilities in China. This method of analysis has its appeals, because we would then be able to determine the effect of anthropogenic transboundary air pollution from Chinese factories and power plants.

However, our research question is to determine the effect of transboundary air pollution from China, which would also include ambient air pollution from the use of coal for heating in winter. Then to capture all the possible paths of pollution flow from China to South Korea, we would ideally simulate forward trajectories from all the coordinates in China. However, we face a number of issues in creating the instrument this way. First, simulating from all the coordinates in China at various heights makes it computationally less tractable. Second, these forward trajectories

²⁶The authors gratefully acknowledge the NOAA Air Resources Laboratory (ARL) for the provision of the HYSPLIT transport and dispersion model and/or READY website (<https://www.ready.noaa.gov>) used in this publication. See [Stein et al. \(2015\)](#) for more information on HYSPLIT.

²⁷For the meteorological data for the HYSPLIT model, we use the NCEP/NCAR Reanalysis data, available from 1948 to present. The NCEP/NCAR Reanalysis data set is a continuously updated globally-gridded data set that is jointly produced by the National Centers for Environmental Prediction (NCEP) and the National Center for Atmospheric Research (NCAR). This data set is a product of a data assimilation project where the initial states of the atmosphere are “reanalyzed” by incorporating historical observations and using a numerical weather prediction (NWP) model from 1948 to present. This data set has a $2.5^\circ \times 2.5^\circ$ spatial resolution with a timestamp of six hours.

Figure A.1: Description of the Trajectory Equation



may not fully capture all the possible paths of transboundary air movements due to discrete starting points of trajectory simulation.

On the other hand, backward trajectory analysis is useful for determining the source locations of pollutants. For our research question, we can track back in time trajectories that are simulated from South Korea to determine whether the trajectories reach China. This method is computationally less intensive than the first method, because trajectories can be simulated from each South Korean city at a given height.

However, this method also has limitations. Simulating backward trajectories with a given duration is based on the assumption that pollutants have traveled for that given duration; that is, we cannot determine whether pollution *originated* from China. This is a valid concern in that we cannot ascertain exact sources of air pollution that arrive at South Korea if there are multiple possible polluting sources in the region. However, this is not a grave concern for our study, because we are interested in knowing whether air pollution in South Korea passed through China, not whether it *originated* from China. It is possible that the transboundary air pollution variable picked up pollution from other neighboring countries of China.

Another limitation is that trajectories of particles from two different source locations may intersect at a city in South Korea, and computing backward trajectories may not correctly identify the source locations. However, this is a limitation of the HYSPLIT model that exists in both forward and backward trajectory analyses. The trajectory calculation relies on the mean wind speed and wind direction at the grid point, and the advection of a particle is computed using the mean of the three-dimensional velocity vectors obtained from the input meteorological conditions. Thus, the trajectory analysis in the HYSPLIT model provides the average locations of the particle back in time, which we believe is a good approximation of the mean locations of the pollutants observed at the pollution monitor in South Korean cities back in time.

One may then ask whether particle dispersion can address our research question better than trajectory calculation. HYSPLIT introduces particle dispersion by calculating the trajectory for many points. However, each trajectory changes its course by the random atmospheric turbulence along its path (where the random shock is provided within the HYSPLIT model), creating dispersion among particles. Due to this method of computation, particle dispersion results in the arrival of fewer particles as the distance between the source and the destination increases. Thus, we decided that computing backward trajectories is the most suitable way to determine whether air pollution in South Korea at a given time passed through China some time ago in expectation.

Construction of instrumental variables using the HYSPLIT model

To construct instrumental variables, we run backward trajectory simulations in the HYSPLIT model. We compute 200-hour backward trajectories 500 meters off the ground every hour for each South Korean city from January 2015 to December 2019, running 9,986,400 trajectories in total ($24 \text{ hourly trajectories/day} \times 365 \text{ days/year} \times 5 \text{ years} \times 228 \text{ cities in South Korea}$).

The height of 500 meters was selected, because if a trajectory starts at a height close to the ground level, it will most likely not travel anywhere. In the atmospheric sciences literature, the height of 850 hPa, which is usually just above the planetary boundary layer (PBL), is typically used for backward trajectory simulations. The idea is that if an air parcel reaches that level, the dynamics of the atmospheric boundary layer will bring it down to the surface. Because the focus of our study is near-surface transport of particulate matter, we do not want to simulate trajectories at an altitude higher than the PBL, the lowest part of the atmosphere directly influenced by the Earth's surface. We decided to choose an altitude below the PBL to capture the air mass dynamics most relevant for near-surface transport.

We also chose a starting height that is sufficiently high within the PBL to avoid local topographic influences yet still capture near-surface transport. If the starting height is too low, the trajectories can be excessively influenced by local surface effects (e.g., topography, vegetation) that occur at lower altitudes, making the trajectory easily hit the ground and lose accuracy. [Ryan et al. \(2023\)](#) state that the mid-boundary-layer starting height (500 m) was chosen as it best represents the source of air in the well-mixed planetary boundary layer. The Kleibergen-Paap rk Wald F-statistics in Table A.10 also provides supporting evidence on this point. The first stage relationship is strongest at 500 meters and becomes substantially weaker at 100 meters.

The main instrument used in this study takes the average value of the $\text{PM}_{2.5}$ concentrations retrieved from the nearest monitors to each hourly trajectory point within China, and 0 otherwise. We define that a trajectory point is within China if the particle enters the boundary layer of China under the specified height (we use 1 km for the default height, but we test other heights for robustness checks) in the duration of 200 hours.

The alternative instrument used for the robustness check takes the value of the $\text{PM}_{2.5}$ concentration retrieved from the final Chinese city that the trajectory passed through before arriving at South Korea, or 0 otherwise.

Appendix B Construction of a city-level dataset

Hourly $\text{PM}_{2.5}$ concentrations in South Korea are obtained from the Korea Environment Corporation’s air pollution data. The data are at the hourly, *monitor* level. To convert the monitor-level data to the city-level data, we take the following steps:

1. Using the coordinates of the monitoring stations, we map monitoring stations onto South Korean cities.
2. We categorize monitoring stations into “good” monitors and “bad” monitors. A “good” monitor is defined as a monitor that has a non-missing rate (in days) higher than 90%, and a “bad” monitor as a monitor that has a non-missing rate lower than 90%.
3. We then categorize South Korean cities, for each date, into three groups: 1) cities that have a good monitor within their boundaries, 2) cities that do not have any good monitors, but only a bad monitor within their boundaries, and 3) cities that do not have any monitor within their boundaries.
4. For cities in the second group or the third group, we impute their missing values with the values from the nearest good monitor. The nearest good monitor of a city is defined as a good monitor outside the city’s boundary that is closest in Euclidean distance from the centroid of the city.
5. When a city has multiple good monitors and bad monitors, we take the average of hourly values across the good monitors. When a city does not have any good monitor but has multiple bad monitors, we take the average of hourly values across the bad monitors.

The same procedure is applied to the South Korean monitor-level meteorological data obtained from the Korea Meteorological Administration. The meteorological data include wind, rainfall, temperature, and humidity levels, some of which are included as control variables in our empirical analysis.

Hourly $\text{PM}_{2.5}$ concentrations in China are obtained from Berkeley Earth. Berkeley Earth collects hourly $\text{PM}_{2.5}$ concentration observations at the city level that are regionally interpolated from real-time observations made by ground-level monitoring stations. Detailed discussion of the interpolation process can be found in [Rohde and Muller \(2015\)](#).

Appendix C Additional Figures and Tables

In this online appendix, we provide additional figures and tables from our analysis.

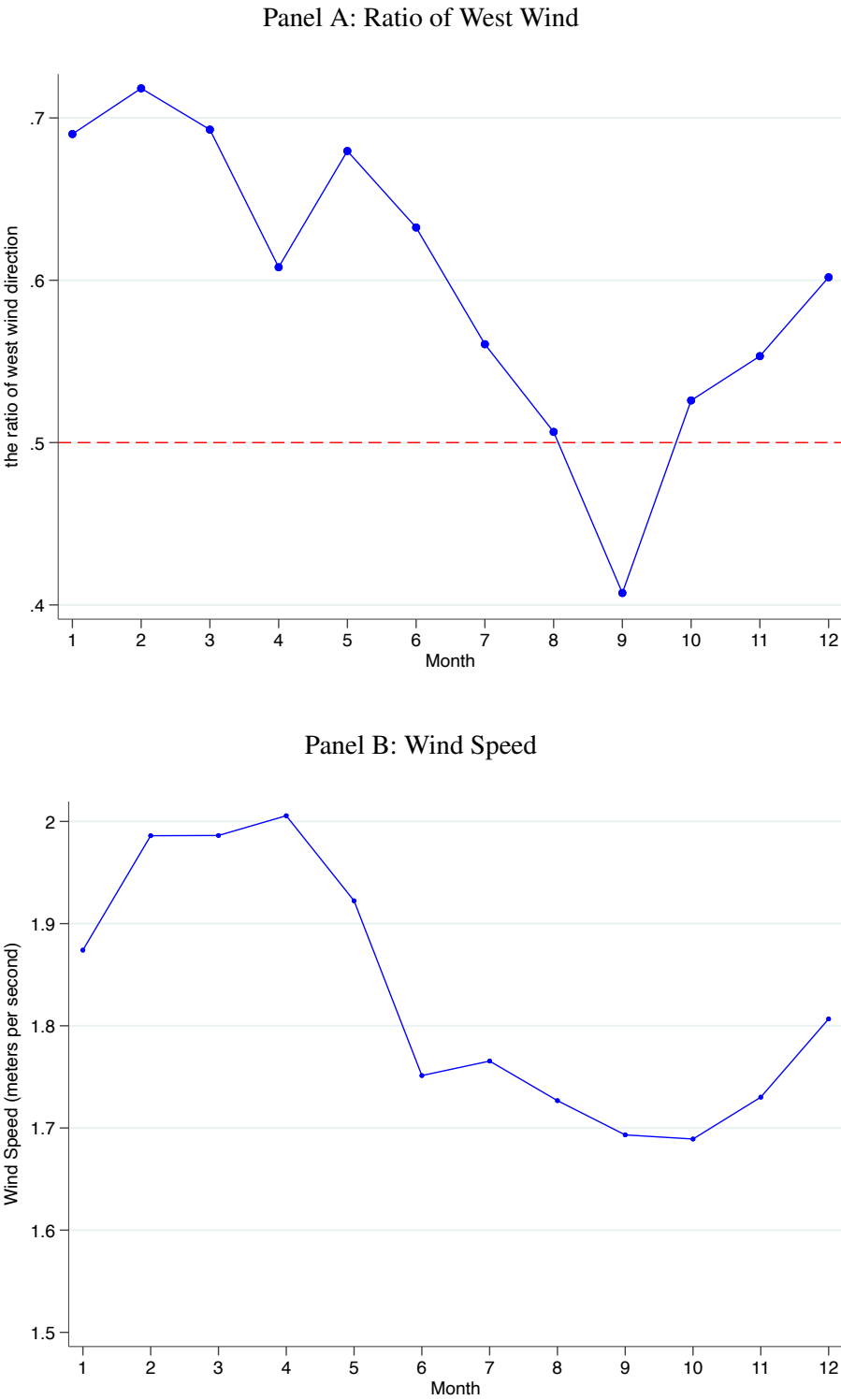
List of Figures in Appendix

A.1	Description of the Trajectory Equation	A-2
A.2	Seasonality in Wind Speed and Direction in Seoul	A-6
A.3	Map of PM _{2.5} Monitor Locations	A-7
A.4	Location of Meteorological Monitoring Stations in South Korea	A-8
A.5	Histogram of the Duration of Trajectories from China to South Korea	A-9

List of Tables in Appendix

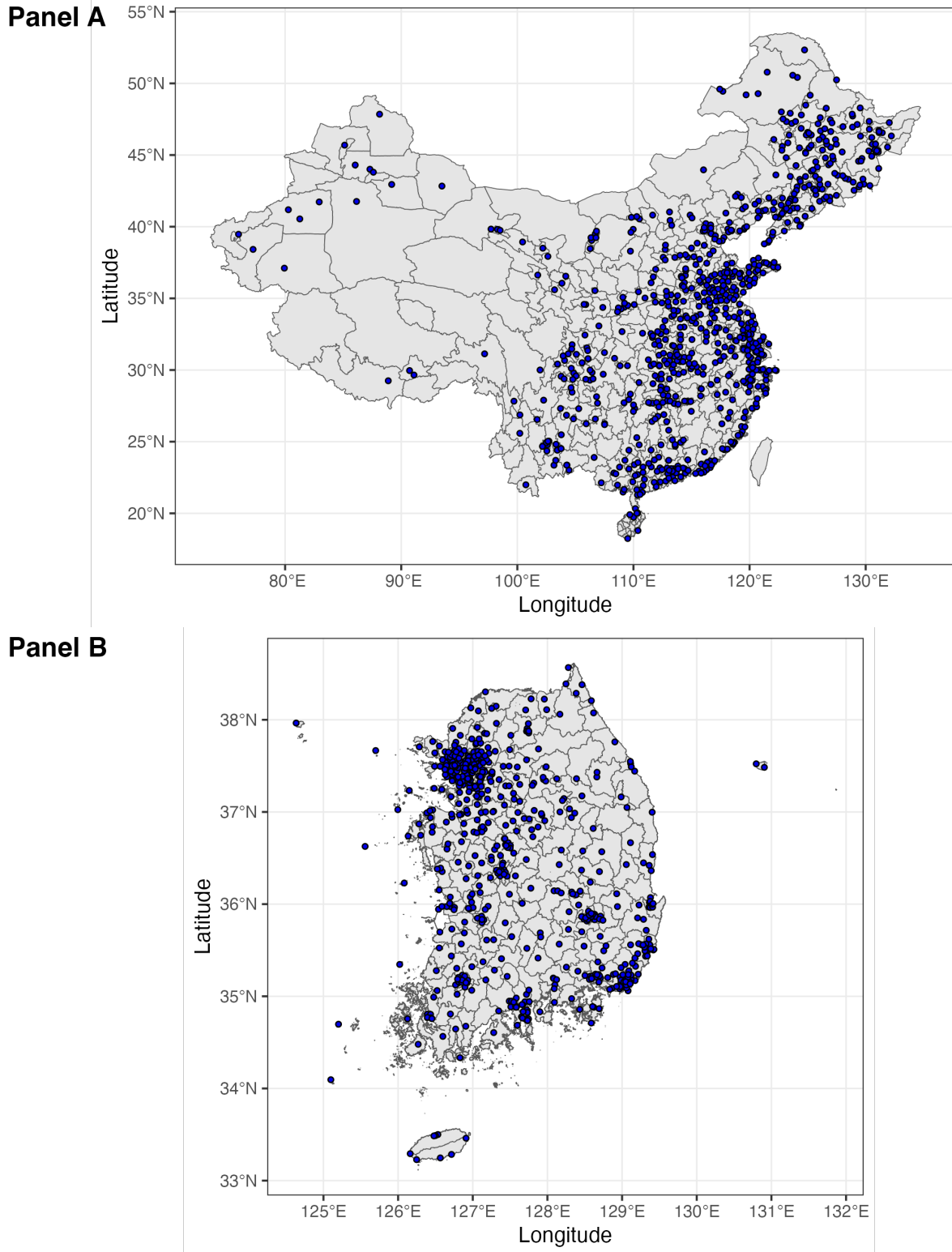
A.1	PM _{2.5} Concentrations by Season and Province	A-10
A.2	Robustness Check on Tables 3 and 4: Average Effect over Past 140 Days	A-11
A.3	Robustness Check on the Instrument: Alternative Instrument Using Only the Last Point in China (First-Stage Regressions of Transboundary Air Pollution on Local Air Quality in South Korea)	A-12
A.4	Robustness Check on the Instrument: Alternative Instrument Using Only the Last Point in China (Impacts of Transboundary Air Pollution on Mortality in South Korea, Reduced-form)	A-13
A.5	Robustness Check on the Instrument: Alternative Instrument Using Only the Last Point in China (Impacts of Local Air Quality on Mortality in South Korean Cities, IV Estimation)	A-14
A.6	Robustness Check on the Instrument: Alternative Instrument Using Only the Last Point in China (Impacts of Transboundary Air Pollution on Mortality by Age Group)	A-15
A.7	Robustness Check on Tables 3 and 4: IV Interacted with Distance	A-16
A.8	Robustness Check for the Choices of Different Control Variables for Reduced Form Estimation	A-17
A.9	Robustness Check for the Choices of Different Control Variables for the IV Estimation	A-18
A.10	Robustness check of HYSPLIT to Choices of Different Starting Heights from South Korea	A-19
A.11	Dependent Variable: PM _{2.5} in China at the city-year-month-day level	A-20
A.12	Dependent Variable: PM _{2.5} in China at the city-year-month-day level	A-21
A.13	Value of remaining life for each age group in South Korea	A-22
A.14	Average economic indicators at province level in 2015	A-23
A.15	Weighted average economic indicators at province level in 2015	A-24

Figure A.2: Seasonality in Wind Speed and Direction in Seoul



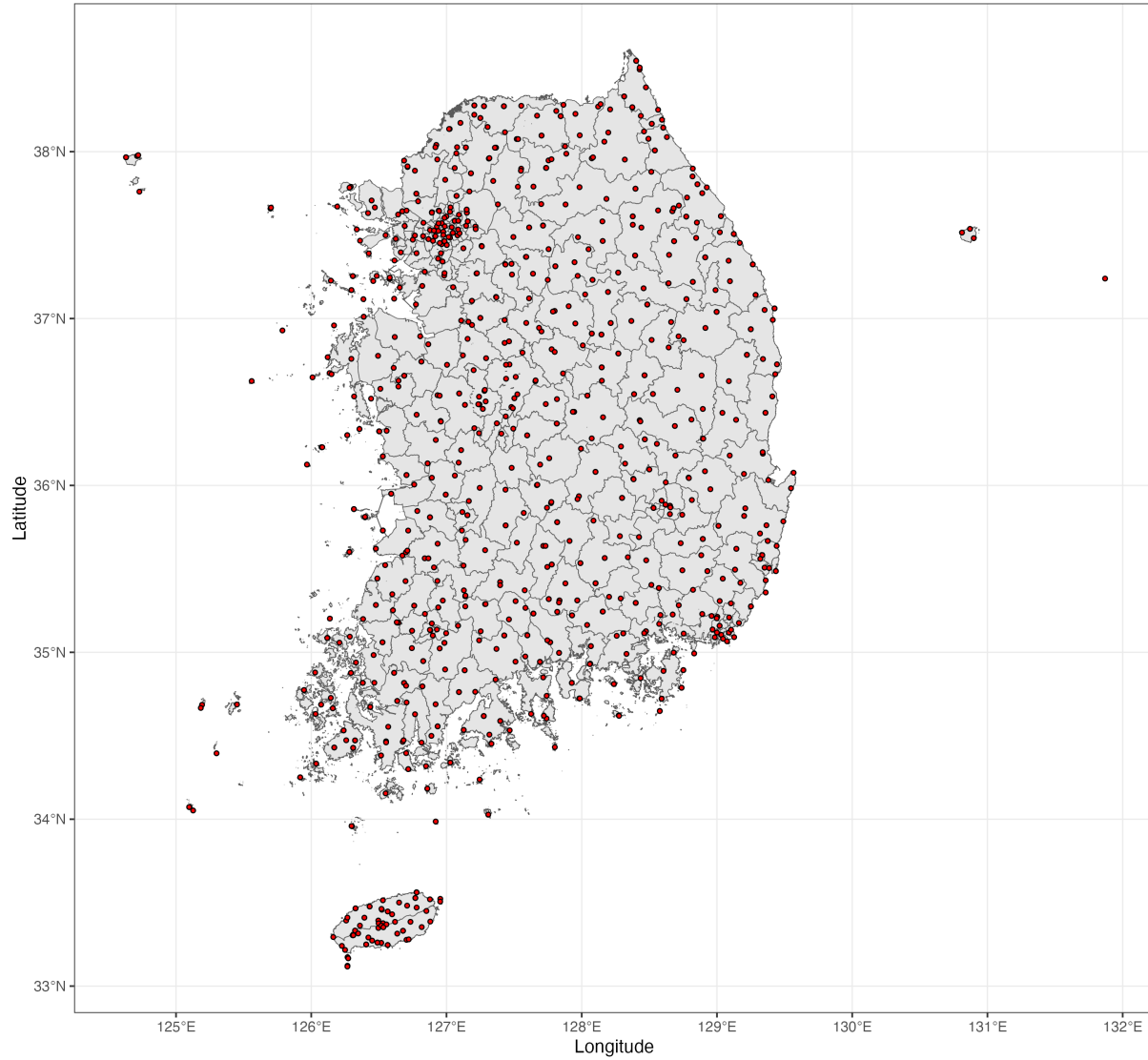
Note: Panel A shows the monthly fraction of hours with westerly winds in Seoul. The sample includes all the meteorological stations in Seoul, South Korea, between January 2015 and December 2019.

Figure A.3: Map of PM_{2.5} Monitor Locations



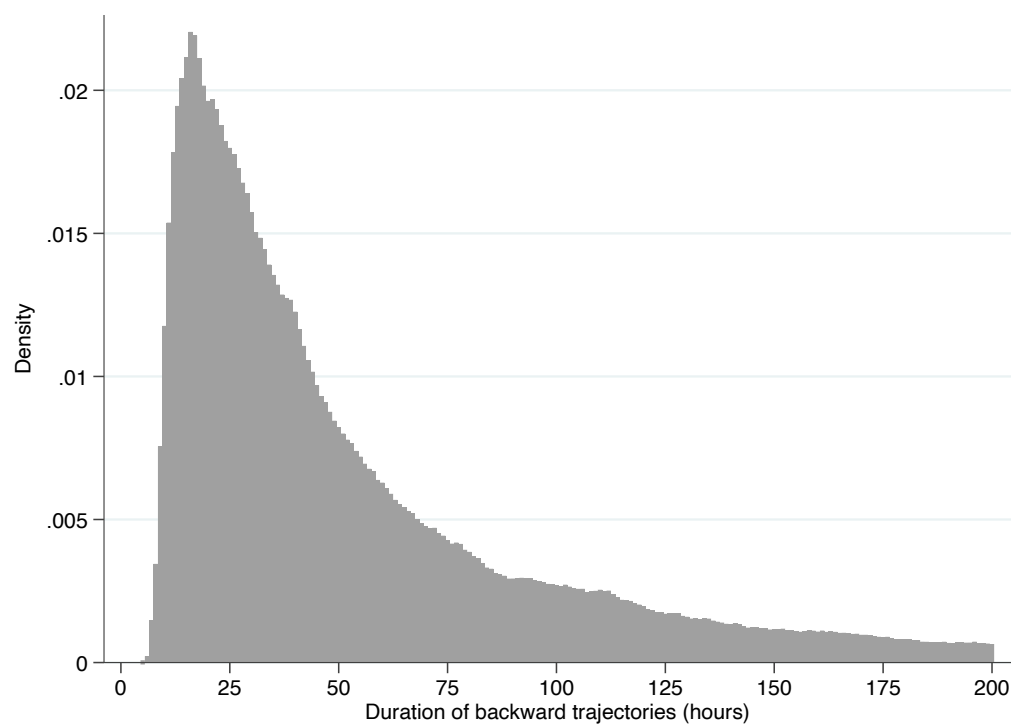
Note: This figure shows the locations of city coordinates available in the Chinese hourly PM_{2.5} concentrations data from Berkeley Earth (Panel A) and the locations of monitors in the South Korean hourly PM_{2.5} concentrations data from the Korea Environment Corporation (Panel B).

Figure A.4: Location of Meteorological Monitoring Stations in South Korea



Note: This figure shows the locations of ground monitoring stations that collect meteorological data in South Korea.

Figure A.5: Histogram of the Duration of Trajectories from China to South Korea



Note: We define the duration of a trajectory as the number of hours it took from the last grid point in China to a city in South Korea. The sample includes trajectories from all South Korean cities between January 2015 and December 2019. The mean is 52 hours, and the median is 38 hours. The 25th percentile is 22 hours, and the 75th percentile is 69 hours.

Table A.1: PM_{2.5} Concentrations by Season and Province

Province	Spring	Summer	Fall	Winter
South Korea				
Busan	28.34	22.13	21.63	28.45
Chungcheongbuk-do	29.5	16.85	24.22	34.37
Chungcheongnam-do	26.31	19.71	25.22	30.87
Daegu	25.39	20.02	22.65	29.83
Daejeon	26.17	16.51	20.91	28.48
Gangwon-do	28.62	18.6	20.07	30.57
Gwangju	25.78	18.86	22.74	26.3
Gyeonggi-do	30.58	18.47	23.08	33.55
Gyeongsangbuk-do	26.15	17.84	21.88	27.74
Gyeongsangnam-do	25.81	21.77	20.55	25.94
Incheon	29.15	21.62	23.42	29.16
Jeju	23.52	17.01	18.1	22.02
Jeollabuk-do	31.84	21.27	27.05	33.38
Jeollanam-do	25.68	20.42	20.81	25.46
Sejong	25.4	18.81	19.74	27.3
Seoul	28.3	20.3	20.7	28.84
Ulsan	28.13	23.25	20.64	25.05
China				
Anhui	52.96	33.04	49.19	81.01
Beijing	58.97	43.09	56.18	77.06
Chongqing	41.73	31.19	39.54	75.36
Fujian	31.25	20.29	24.3	35.48
Gansu	39.19	26.39	32.32	53.25
Guangdong	31.97	21.35	33.29	44.03
Guangxi	36.09	23.52	35.44	54.8
Guizhou	34.34	22.19	30.01	48.53
Hainan	21.69	13.37	20.53	29.16
Hebei	60.99	46.93	62.16	97.66
Heilongjiang	33.55	19.67	36.27	52.41
Henan	63.15	41.88	59.75	111.45
Hubei	51.77	32.43	47.62	89.75
Hunan	43.25	27.97	43.51	72.01
Inner Mongolia	32.11	23.93	30.93	42.54
Jiangsu	51.55	33.27	43.17	76.26
Jiangxi	40.41	27.19	38.98	60.22
Jilin	38.63	22.61	39.55	59.39
Liaoning	45.51	29.36	43.94	62.56
Ningxia Hui Autonomous Region	43.87	32.22	44.12	61.5
Qinghai	43	29.9	39.32	62.99
Shaanxi	49.16	32.18	50.34	96.04
Shandong	57.5	37.97	55.16	92.17
Shanghai	47.04	32.73	37	62.76
Shanxi	52.63	41.77	54.48	87.54
Sichuan	44.03	28.74	38.03	74.6
Tianjin	62.84	46.11	61.11	85.08
Tibet	22.53	15.25	20.13	27.89
Xinjiang	62.22	34.79	43.65	76.96
Yunnan	32.04	18.95	22.76	31.77
Zhejiang	41.82	26.54	34.16	57.99

Table A.2: Robustness Check on Tables 3 and 4: Average Effect over Past 140 Days

Panel A: Reduced-form Estimation (Dependent variable: hourly mortality per billion)				
	Overall	Elderly	Infant	Respiratory/ cardiovascular
Transboundary PM _{2.5} (past 0-140 days)	4.02 (0.75)	20.04 (5.03)	7.53 (4.31)	1.68 (0.18)
Mean of dependent variable	618	3,250	314	149
Marginal effect on mortality (%)	0.7%	0.6%	2.4%	1.1%
Marginal effect on annual mortality/million	35.2	175.6	66.0	14.7
Panel B: IV Estimation (Dependent variable: hourly mortality per billion)				
	Overall	Elderly	Infant	Respiratory/ cardiovascular
PM _{2.5} (past 0-140 days)	7.75 (1.47)	38.62 (9.77)	14.48 (8.25)	3.23 (0.36)
Mean of dependent variable	618	3,250	314	149
Marginal effect on mortality (%)	1.3%	1.2%	4.6%	2.2%
Marginal effect on annual mortality/million	67.9	338.3	126.9	28.3

Note: Panel A shows OLS estimation results for equation (2). Panel B shows IV estimation results for equation (3). Two-way cluster-robust standard errors at the city and hour levels are reported in parentheses. The dependent variable is hourly mortality per billion people in each category. In the OLS estimation, all groups have 9,177,203 observations. In the IV estimation, all groups have 9,172,016 observations. All regressions include city-by-year-by-month fixed effects, city-by-day of week fixed effects, city-by-rainfall quartile fixed effects, city-by-temperature quartile fixed effects, and are weighted by city-level population. The Kleibergen-Paap rk Wald F statistic is 1,260 for all columns in Panel B. The sample includes all South Korean cities between January 2015 and December 2019.

Table A.3: Robustness Check on the Instrument: Alternative Instrument Using Only the Last Point in China (First-Stage Regressions of Transboundary Air Pollution on Local Air Quality in South Korea)

	(1)	(2)	(3)	(4)
Hourly Transboundary PM _{2.5}	0.170 (0.003)	0.129 (0.002)	0.129 (0.002)	0.129 (0.002)
Constant	22.774 (0.325)			
Observations	9,161,475	9,108,372	9,108,372	9,108,372
KP F-stat	2521	3111	3344	3273
Year-Month-City FE	No	No	Yes	Yes
Year-Month FE	No	Yes	No	No
Month-City FE	No	Yes	No	No
Month-Province FE	No	No	No	No
City FE	Yes	Yes	Yes	Yes
Day of week-City FE	No	Yes	Yes	Yes
Rainfall quartile-City FE	No	Yes	No	Yes
Temperature quartile-City FE	No	Yes	No	Yes
Rainfall quartile FE	No	No	Yes	No
Temperature quartile FE	No	No	Yes	No

Note: The alternative instrumental variable used in this set of regressions takes the values as follows. If the 200-hour backward trajectory does not reach China, then it takes a value of 0. If it reaches China, then all the hourly trajectory points are matched with the nearest pollution monitors in China. The instrument takes the average of all the PM_{2.5} values collected from the nearest Chinese monitors for each trajectory point. This table shows OLS estimation results for equation (1) using this alternative instrument. Two-way cluster-robust standard errors at the city and hour levels are reported in parentheses. The dependent variable is hourly mortality per billion people in each category. The first specification has 9,342,033 observations, and the rest have 9,287,734 observations. The sample periods are from January 2015 to December 2019.

Table A.4: Robustness Check on the Instrument: Alternative Instrument Using Only the Last Point in China (Impacts of Transboundary Air Pollution on Mortality in South Korea, Reduced-form)

Panel A: Average Effect Over Past 70 Days (Dependent variable: hourly mortality per billion people)				
	Overall	Elderly	Infant	Respiratory/ cardiovascular
Transboundary PM _{2.5} (past 0-70 days)	3.56 (0.57)	19.00 (3.88)	6.68 (2.58)	1.66 (0.23)
Observations	9,555,368	9,555,368	9,555,368	9,555,368
Mean of dependent variable	618	3,259	314	148
Marginal effect on mortality (%)	0.6%	0.6%	2.1%	1.1%
Marginal effect on annual mortality/million	31.2	166.5	58.5	14.5
Panel B: Weekly Lagged Effects (Dependent variable: hourly mortality per billion people)				
	Overall	Elderly	Infant	Respiratory/ cardiovascular
Transboundary PM _{2.5} (past 0-7 day)	0.28 (0.10)	1.35 (0.65)	0.90 (0.58)	0.14 (0.04)
Transboundary PM _{2.5} (past 7-14 day)	0.34 (0.08)	1.93 (0.58)	0.37 (0.66)	0.21 (0.04)
Transboundary PM _{2.5} (past 14-21 day)	0.55 (0.11)	3.16 (0.65)	2.02 (0.69)	0.25 (0.05)
Transboundary PM _{2.5} (past 21-28 day)	0.60 (0.11)	3.59 (0.66)	-0.36 (0.43)	0.25 (0.05)
Transboundary PM _{2.5} (past 28-35 day)	0.62 (0.11)	3.61 (0.80)	1.18 (0.69)	0.23 (0.05)
Transboundary PM _{2.5} (past 35-42 day)	0.66 (0.12)	3.81 (0.68)	0.10 (0.74)	0.27 (0.05)
Transboundary PM _{2.5} (past 42-49 day)	0.47 (0.11)	2.42 (0.63)	1.21 (0.74)	0.14 (0.05)
Transboundary PM _{2.5} (past 49-56 day)	0.61 (0.07)	3.50 (0.56)	0.87 (0.72)	0.22 (0.03)
Transboundary PM _{2.5} (past 56-63 day)	0.29 (0.06)	1.74 (0.44)	0.42 (0.40)	0.12 (0.02)
Transboundary PM _{2.5} (past 63-70 day)	0.07 (0.06)	-0.09 (0.41)	0.67 (0.67)	0.09 (0.02)
Observations	9,555,318	9,555,318	9,555,318	9,555,318
Mean of dependent variable	618	3,259	314	148

Note: This table shows OLS estimation results for equation (2). Two-way cluster-robust standard errors at the city and hour levels are reported in parentheses. All regressions include city-by-year-by-month fixed effects, city-by-day of week fixed effects, city-by-rainfall quartile fixed effects, city-by-temperature quartile fixed effects, and are weighted by city-level population. The sample includes all South Korean cities between January 2015 and December 2019.

Table A.5: Robustness Check on the Instrument: Alternative Instrument Using Only the Last Point in China (Impacts of Local Air Quality on Mortality in South Korean Cities, IV Estimation)

Panel A: Average Effect Over the Past 70 Days (Dependent variable: hourly mortality per billion people)				
	Overall	Elderly	Infant	Respiratory/ cardiovascular
PM _{2.5} (past 0-70 days)	9.10 (1.48)	48.63 (9.91)	17.47 (6.79)	4.24 (0.58)
Mean of dependent variable	618	3,258	314	148
Marginal effect on mortality (%)	1.5%	1.5%	5.6%	2.9%
Marginal effect on annual mortality/million	79.7	426.0	153.0	37.2
Panel B: Weekly Lagged Effects (Dependent variable: hourly mortality per billion people)				
	Overall	Elderly	Infant	Respiratory/ cardiovascular
PM _{2.5} (past 0-7 days)	0.78 (0.29)	4.05 (1.83)	2.08 (1.69)	0.37 (0.09)
PM _{2.5} (past 7-14 days)	0.69 (0.20)	3.68 (1.34)	0.25 (1.68)	0.52 (0.09)
PM _{2.5} (past 14-21 days)	1.23 (0.31)	7.10 (1.89)	5.15 (2.09)	0.62 (0.14)
PM _{2.5} (past 21-28 days)	1.37 (0.28)	8.23 (1.69)	-1.41 (1.52)	0.67 (0.12)
PM _{2.5} (past 28-35 days)	1.31 (0.28)	7.88 (1.92)	3.49 (1.62)	0.51 (0.11)
PM _{2.5} (past 35-42 days)	1.63 (0.29)	9.77 (1.56)	0.12 (1.87)	0.66 (0.12)
PM _{2.5} (past 42-49 days)	1.37 (0.33)	7.50 (2.05)	3.01 (2.02)	0.43 (0.15)
PM _{2.5} (past 49-56 days)	2.23 (0.29)	13.01 (1.88)	3.79 (2.40)	0.78 (0.13)
PM _{2.5} (past 56-63 days)	1.42 (0.25)	8.94 (1.53)	1.12 (1.30)	0.49 (0.10)
PM _{2.5} (past 63-70 days)	0.20 (0.14)	-0.03 (1.15)	2.11 (1.64)	0.21 (0.07)
Mean of dependent variable	617	3,260	315	148

Note: This table shows instrumental variable estimation results for equation (3). Two-way cluster-robust standard errors at the city and hour levels are reported in parentheses. All groups in Panel A have 9,528,960 observations, and all groups in Panel B have 9,274,063 observations. All columns include city-by-year-by-month fixed effects, city-by-day of week fixed effects, city-by-rainfall quartile fixed effects, city-by-temperature quartile fixed effects, and are weighted by city-level population. The Kleibergen-Paap rk Wald F statistic is 1,816 for all columns in Panel A and 356 for all columns in Panel B.

Table A.6: Robustness Check on the Instrument: Alternative Instrument Using Only the Last Point in China (Impacts of Transboundary Air Pollution on Mortality by Age Group)

Panel A: Reduced Form (Dependent variable: hourly mortality per billion people)						
	Infant	1-9	10-19	20-29	30-39	40-49
Transboundary PM _{2.5} (past 0-70 days)	6.68 (2.58)	0.18 (0.22)	-0.14 (0.18)	0.04 (0.19)	0.94 (0.40)	0.61 (0.34)
Mean of dependent variable	314	12	18	42	79	169
Marginal effect as % increase in mortality	2.1%	1.5%	-0.8%	0.1%	1.2%	0.4%
Marginal effect on annual mortality/million	58.6	1.6	-1.3	0.3	8.2	5.3
	50-59	60-69	70-79	80-89	90-99	100-109
Transboundary PM _{2.5} (past 0-70 days)	2.70 (0.62)	4.60 (1.17)	13.85 (3.86)	39.63 (10.09)	110.42 (41.15)	185.48 (174.13)
Mean of dependent variable	364	746	2313	7324	19368	16318
Marginal effect as % increase in mortality	0.7%	0.6%	0.6%	0.5%	0.6%	1.1%
Marginal effect on annual mortality/million	23.6	40.3	121.3	347.1	967.3	1624.8
Panel B: IV Estimation (Dependent variable: hourly mortality per billion people)						
	Infant	1-9	10-19	20-29	30-39	40-49
PM _{2.5} (past 0-70 days)	17.48 (6.79)	0.46 (0.58)	-0.35 (0.47)	0.09 (0.51)	2.43 (1.03)	1.61 (0.89)
Mean of dependent variable	314	12	18	42	79	169
Marginal effect as % increase in mortality	5.6%	3.7%	-2.0%	0.2%	3.1%	0.9%
Marginal effect on annual mortality/million	153.1	4.0	-3.1	0.8	21.3	14.1
	50-59	60-69	70-79	80-89	90-99	100-109
PM _{2.5} (past 0-70 days)	6.93 (1.68)	11.62 (3.03)	35.13 (9.97)	101.91 (26.21)	285.67 (104.98)	467.04 (443.11)
Mean of dependent variable	364	746	2312	7322	19365	16323
Marginal effect as % increase in mortality	1.9%	1.6%	1.5%	1.4%	1.5%	2.9%
Marginal effect on annual mortality/million	60.7	101.8	307.7	892.8	2502.5	4091.3

Note: Panel A shows age-specific results for the OLS estimation in equation (2), and Panel B shows results for the instrumental variable estimation in equation (3). Two-way cluster-robust standard errors at the city and hour levels are reported in parentheses. In the OLS estimation, all age groups have 9,555,368 observations, except for the age group 100-109, which has 9,537,950 observations. The age group 100-109 has fewer observations because the population for age over 100 is 0 for some years in some cities in the sample. In the IV estimation, all age groups have 9,528,950 observations, except for the age group 100-109, which has 9,511,542 observations. All regressions include city-by-year-by-month fixed effects, city-by-day of week fixed effects, city-by-rainfall quartile fixed effects, city-by-temperature quartile fixed effects, and are weighted by city-level population. The Kleibergen-Paap rk Wald F statistic for Panel B is 1,814 for all age groups except for age group 100-109 (1,825). The sample includes all South Korean cities between January 2015 and December 2019.

Table A.7: Robustness Check on on Tables 3 and 4: IV Interacted with Distance

Panel A: Impacts of Transboundary Air Pollution on Local Air Quality in South Korea (First-Stage Regressions)

	(1)	(2)	(3)	(4)
Hourly Transboundary PM _{2.5}	0.195 (0.005)	0.142 (0.002)	0.143 (0.002)	0.143 (0.002)
Hourly Transboundary PM _{2.5} × Distance	-0.038 (0.005)	-0.018 (0.003)	-0.020 (0.003)	-0.020 (0.003)
Constant	22.393 (0.311)			
Observations	9,159,814	9,106,739	9,106,739	9,106,739
KP F-stat	1462	1969	2230	2178
Year-Month-City FE	No	No	Yes	Yes
Year-Month FE	No	Yes	No	No
Month-City FE	No	Yes	No	No
Month-Province FE	No	No	No	No
City FE	Yes	Yes	Yes	Yes
Day of week-City FE	No	Yes	Yes	Yes
Rainfall quartile-City FE	No	Yes	No	Yes
Temperature quartile-City FE	No	Yes	No	Yes
Rainfall quartile FE	No	No	Yes	No
Temperature quartile FE	No	No	Yes	No

Panel B: Impacts of Local Air Quality on Mortality (2SLS Estimation)

	Overall	Elderly	Infant	Respiratory/ cardiovascular
PM _{2.5} (past 0-70 days)	8.68 (1.60)	44.83 (10.38)	19.49 (7.51)	4.13 (0.57)
Observations	9,528,960	9,528,960	9,528,960	9,528,960
Mean of dependent variable	618	3,258	314	148
Marginal effect on mortality (%)	1.4%	1.4%	6.2%	2.8%
Marginal effect on annual mortality/million	76.0	392.7	170.8	36.2

Note: The additional instrumental variable used in this set of regressions takes the values as follows. If the 200-hour backward trajectory does not reach China, then it takes a value of 0. If it reaches China, then it takes the value of the PM_{2.5} level from the nearest Chinese monitor multiplied by the demeaned distance (in 1000 km) of the trajectory from the starting point to the first arrival point of the backward trajectory in China. This table shows OLS estimation results for equation (1) using this alternative instrument. Two-way cluster-robust standard errors at the city and hour levels are reported in parentheses. The dependent variable is hourly mortality per billion people in each category. The sample periods are from January 2015 to December 2019.

Table A.8: Robustness Check for the Choices of Different Control Variables for Reduced Form Estimation

	(1)	(2)	(3)	(4)
Transboundary PM _{2.5} (past 0-7 days)	0.26 (0.10)	0.26 (0.10)	0.17 (0.10)	0.18 (0.10)
Transboundary PM _{2.5} (past 7-14 days)	0.35 (0.08)	0.35 (0.09)	0.24 (0.07)	0.24 (0.07)
Transboundary PM _{2.5} (past 14-21 days)	0.57 (0.11)	0.57 (0.11)	0.41 (0.09)	0.40 (0.09)
Transboundary PM _{2.5} (past 21-28 days)	0.57 (0.11)	0.59 (0.11)	0.41 (0.08)	0.39 (0.08)
Transboundary PM _{2.5} (past 28-35 days)	0.61 (0.12)	0.62 (0.12)	0.42 (0.10)	0.39 (0.10)
Transboundary PM _{2.5} (past 35-42 days)	0.69 (0.12)	0.70 (0.13)	0.50 (0.10)	0.47 (0.10)
Transboundary PM _{2.5} (past 42-49 days)	0.45 (0.11)	0.45 (0.11)	0.28 (0.08)	0.24 (0.08)
Transboundary PM _{2.5} (past 49-56 days)	0.60 (0.08)	0.61 (0.08)	0.46 (0.07)	0.43 (0.07)
Transboundary PM _{2.5} (past 56-63 days)	0.28 (0.06)	0.29 (0.06)	0.20 (0.05)	0.20 (0.05)
Transboundary PM _{2.5} (past 63-70 days)	0.05 (0.06)	0.05 (0.06)	-0.00 (0.07)	-0.00 (0.06)
Observations	9,555,368	9,555,368	9,555,368	9,555,368
Dependent variable mean	618	618	618	618
Year-Month-City FE	Yes	Yes	No	No
Year-Month FE	No	No	Yes	Yes
Month-City FE	No	No	Yes	No
Month-Province FE	No	No	No	Yes
Year FE	No	No	No	No
Month FE	No	No	No	No
City FE	Yes	Yes	Yes	Yes
Day of week-City FE	Yes	Yes	Yes	No
Rainfall quartile-City FE	Yes	No	Yes	Yes
Temperature quartile-City FE	Yes	No	Yes	Yes
Rainfall quartile FE	No	Yes	No	No
Temperature quartile FE	No	Yes	No	No

Note: This table shows results for Column 1 in Table 3 with different choices of control variables. See notes in Table 3. Column 1 in this table replicates Column 1 in Table 3, and we show results with different choices of control variables in columns 2 to 4.

Table A.9: Robustness Check for the Choices of Different Control Variables for the IV Estimation

	(1)	(2)	(3)	(4)
PM _{2.5} (past 0-7 days)	0.55 (0.29)	0.56 (0.30)	0.58 (0.31)	0.57 (0.30)
PM _{2.5} (past 7-14 days)	0.73 (0.23)	0.73 (0.24)	0.76 (0.23)	0.73 (0.23)
PM _{2.5} (past 14-21 days)	1.40 (0.35)	1.41 (0.35)	1.41 (0.38)	1.35 (0.37)
PM _{2.5} (past 21-28 days)	1.33 (0.30)	1.37 (0.31)	1.37 (0.31)	1.32 (0.30)
PM _{2.5} (past 28-35 days)	1.33 (0.28)	1.35 (0.28)	1.30 (0.34)	1.18 (0.33)
PM _{2.5} (past 35-42 days)	1.85 (0.32)	1.89 (0.32)	1.79 (0.33)	1.63 (0.32)
PM _{2.5} (past 42-49 days)	1.55 (0.35)	1.57 (0.36)	1.44 (0.39)	1.25 (0.36)
PM _{2.5} (past 49-56 days)	2.36 (0.30)	2.38 (0.31)	2.22 (0.37)	2.03 (0.35)
PM _{2.5} (past 56-63 days)	1.46 (0.23)	1.49 (0.24)	1.44 (0.29)	1.33 (0.27)
PM _{2.5} (past 63-70 days)	0.05 (0.15)	0.06 (0.15)	0.07 (0.20)	0.03 (0.19)
Observations	9,274,113	9,274,113	9,274,113	9,274,113
Dependent variable mean	617	617	617	617
KP F-stat	221	221	8	9
Year-Month-City FE	Yes	Yes	No	No
Year-Month FE	No	No	Yes	Yes
Month-City FE	No	No	Yes	No
Month-Province FE	No	No	No	Yes
Year FE	No	No	No	No
Month FE	No	No	No	No
City FE	Yes	Yes	Yes	Yes
Day of week-City FE	Yes	Yes	Yes	No
Rainfall quartile-City FE	Yes	No	Yes	Yes
Temperature quartile-City FE	Yes	No	Yes	Yes
Rainfall quartile FE	No	Yes	No	No
Temperature quartile FE	No	Yes	No	No

Note: This table shows results for Column 1 in Table 4 with different choices of control variables. See notes in Table 4. Column 1 in this table replicates Column 1 in Table 4, and we show results with different choices of control variables in columns 2 to 4.

Table A.10: Robustness check of HYSPLIT to Choices of Different Starting Heights from South Korea

Dependent variable: Hourly PM _{2.5} in South Korean cities					
	(1)	(2)	(3)	(4)	(5)
Hourly Transboundary PM _{2.5} (from 100m)	0.049 (0.003)				
Hourly Transboundary PM _{2.5} (from 250m)		0.069 (0.002)			
Hourly Transboundary PM _{2.5} (from 500m)			0.100 (0.003)		
Hourly Transboundary PM _{2.5} (from 750m)				0.117 (0.003)	
Hourly Transboundary PM _{2.5} (from 1000m)					0.110 (0.004)
Observations	1553456	1560982	1573289	1585100	1593754
KP F-stat	355	1023	1560	1551	978

Note: Standard errors, clustered by city, are reported in parentheses. All regressions include city-by-year-by-month fixed effects, city-by-day of week fixed effects, city-by-rainfall quartile fixed effects, city-by-temperature quartile fixed effects, and are weighted by city-level population. KP F-stat is Kleibergen-Paap rk Wald F statistic. The sample includes the 50 cities with the highest number of deaths (in 2018) between March 2015 and December 2018.

Table A.11: Dependent Variable: PM_{2.5} in China at the city-year-month-day level

	(1)	(2)	(3)	(4)
Annual trend	-4.29 (0.12)		-2.52 (0.16)	
Annual trend \times in-China ratio	-8.70 (0.98)	-8.69 (0.98)		
Annual trend \times Quartile 2 of in-China ratio			-1.71 (0.21)	-1.71 (0.21)
Annual trend \times Quartile 3 of in-China ratio			-1.70 (0.28)	-1.71 (0.28)
Annual trend \times Quartile 4 of in-China ratio			-3.52 (0.36)	-3.51 (0.36)
N	1328053	1328026	1328053	1328026
Mean of dependent variable	47.83	47.83	47.83	47.83
City FE	Yes	Yes	Yes	Yes
Time FE	No	Yes	No	Yes

Note: The in-China ratio is divided into quartile groups for columns (3) and (4). Quartile 1 has the lowest in-China ratio. Standard errors, clustered by city, are reported in parentheses. The time fixed effect is at the level of year-month-day. All regressions are weighted by city-level population. The sample includes all South Korean cities between January 2015 and December 2019.

Table A.12: Dependent Variable: PM_{2.5} in China at the city-year-month-day level

	(1)	(2)	(3)	(4)
Annual trend	-3.72 (0.37)		-1.81 (0.19)	
Annual trend \times in-China ratio	-5.60 (1.78)	-5.60 (1.78)		
Annual trend \times Quartile 2 of in-China ratio			-2.26 (0.27)	-2.25 (0.27)
Annual trend \times Quartile 3 of in-China ratio			-2.41 (0.33)	-2.43 (0.33)
Annual trend \times Quartile 4 of in-China ratio			-3.31 (0.62)	-3.30 (0.62)
Annual trend \times 2015 Crude Oil Production	0.02 (0.01)	0.02 (0.01)	0.02 (0.01)	0.02 (0.01)
Annual trend \times 2015 Coke Production	-0.04 (0.02)	-0.04 (0.02)	-0.03 (0.02)	-0.03 (0.02)
N	989924	989897	989924	989897
Mean of dependent variable	49.76	49.76	49.76	49.76
City FE	Yes	Yes	Yes	Yes
Time FE	No	Yes	No	Yes

Note: The in-China ratio is divided into quartile groups for columns (3) and (4). Quartile 1 has the lowest in-China ratio. Standard errors, clustered by city, are reported in parentheses. The time fixed effect is at the level of year-month-day. All regressions are weighted by city-level population. The sample includes all South Korean cities between January 2015 and December 2019.

Table A.13: Value of remaining life for each age group in South Korea

Age Group	VSL
0 (infant)	509,122
1 – 9	519,632
10 – 19	542,066
20 – 29	569,630
30 – 39	559,651
40 – 49	488,678
50 – 59	366,400
60 – 69	233,030
70 – 79	124,647
80 – 89	57,094
90 – 99	23,995
100 – 109	10,200

Note: The values of remaining life for each group are obtained from Figure 3 in [Murphy and Topel \(2006\)](#). The figure includes values of remaining life by sex for each age between 0 and 110, using the mean VSL value of \$6.3 million. These age-specific VSL estimates are averaged within each age group, divided by the mean VSL value of \$6.3 million, and then multiplied by the average South Korean VSL estimate obtained in [4.1](#). The VSL estimates are in 2019 US dollars.

Table A.14: Average economic indicators at province level in 2015

	Group 1	Group 2	Group 3	Group 4
Average China arrival dummy in 2015	0.431	0.535	0.640	0.739
Average PM 2.5 in 2015	39.63	45.86	52.73	62.89
GDP in 2015 (Billion USD)	407.92	324.59	334.01	372.44
GDP per capita in 2015 (Thousand USD)	7.16	8.39	6.93	9.52
VA in primary industry (Billion USD)	34.00	24.45	31.98	29.17
VA in secondary industry (Billion USD)	182.27	137.71	150.19	147.00
VA in tertiary industry (Billion USD)	191.65	162.43	151.84	196.26
VA in agriculture forestry animal husbandry and fishery (Billion USD)	35.10	25.14	33.32	30.38
VA in industrial production (Billion USD)	154.23	115.52	126.60	124.55
VA in construction (Billion USD)	28.35	22.79	24.31	23.00
VA in wholesale (Billion USD)	40.08	34.11	28.98	39.45
VA in transportation and mailing (Billion USD)	16.66	13.70	14.42	20.53
VA in accomodation and food (Billion USD)	8.49	7.15	5.81	5.38
VA in finance (Billion USD)	28.25	24.65	21.45	30.32
VA in real estate (Billion USD)	23.42	19.74	19.44	22.07
VA in other industries (Billion USD)	73.35	61.80	59.68	76.76
Population in 2015 (Million)	53.77	37.94	42.00	44.48
Population (Urban) in 2015 (Million)	30.17	21.78	23.23	27.06
Population (Rural) in 2015 (Million)	23.60	16.16	18.76	17.42
Employment (Urban) in 2015 (Million)	6.52	4.92	5.75	6.16
Income per person (Thousand USD)	3.15	3.78	2.99	4.25
Income (Urban) per person (Thousand USD)	4.58	5.08	4.29	5.33
Income (Rural) per person (Thousand USD)	1.70	2.09	1.68	2.19
Spending per person (Thousand USD)	2.30	2.71	2.21	3.02
Spending (Urban) per person (Thousand USD)	3.13	3.51	3.04	3.66
Spending (Rural) per person (Thousand USD)	1.43	1.66	1.38	1.73
Export + Import in 2015 (Billion USD)	178.16	119.68	90.14	121.31
Export in 2015 (Billion USD)	114.72	71.60	54.43	49.64
Import in 2015 (Billion USD)	63.44	48.08	35.71	71.68
Electricity Supply in 2015 (Billion Kwh)	182.25	152.61	188.62	232.43
Electricity Supply (Hydro) in 2015 (Billion Kwh)	69.99	66.99	11.15	1.75
Electricity Supply (Thermal) in 2015 (Billion Kwh)	95.89	84.11	164.07	212.78
Electricity Demand in 2015 (Billion Kwh)	181.50	140.35	185.93	233.01
Coke production in 2015 (Million Ton)	5.69	8.02	16.30	38.70
Crude production in 2015 (Million Ton)	8.12	0.69	14.65	15.54
Petrol production in 2015 (Million Ton)	3.56	2.75	3.93	7.01
Kerosene production in 2015 (Million Ton)	2.21	1.34	0.93	1.67
Diesel production in 2015 (Million Ton)	6.03	4.17	5.53	12.75
Fuel oil production in 2015 (Million Ton)	0.61	0.32	0.65	2.11
Natural gas production in 2015 (Million Ton)	0.26	0.67	1.10	0.16
Coal consumption in 2015 (Million Ton)	94.66	82.66	156.71	237.89
Coke consumption in 2015 (Million Ton)	7.08	8.93	12.47	27.34
Crude consumption in 2015 (Million Ton)	14.18	13.75	17.84	32.84
Petrol consumption in 2015 (Million Ton)	4.49	5.07	3.62	4.55
Kerosene consumption in 2015 (Million Ton)	0.86	1.53	0.36	1.15
Diesel consumption in 2015 (Million Ton)	6.70	5.78	5.09	6.75
Fuel oil consumption in 2015 (Million Ton)	0.91	1.72	0.55	5.31
Natural gas consumption in 2015 (Million Ton)	0.44	0.71	0.72	0.75

Note: Provinces are divided into quartile groups based on their average in-China ratio. Group 1 has the lowest in-China ratio. Economic data are sourced from the National Bureau of Statistics. Values are converted from CNY to USD using an exchange rate of 6.227. VA = value added.

Table A.15: Weighted average economic indicators at province level in 2015

	Group 1	Group 2	Group 3	Group 4
Average China arrival dummy in 2015	0.426	0.527	0.638	0.744
Average PM 2.5 in 2015	39.07	52.62	58.73	65.96
GDP in 2015 (Billion USD)	549.90	476.69	539.68	500.40
GDP per capita in 2015 (Thousand USD)	7.62	8.58	7.96	8.39
VA in primary industry (Billion USD)	38.16	39.33	46.00	44.94
VA in secondary industry (Billion USD)	246.66	210.60	250.53	213.02
VA in tertiary industry (Billion USD)	265.07	226.76	243.15	242.45
VA in agriculture forestry animal husbandry and fishery (Billion USD)	39.38	40.42	47.96	46.87
VA in industrial production (Billion USD)	215.88	176.34	211.97	181.83
VA in construction (Billion USD)	31.27	35.20	39.34	31.90
VA in wholesale (Billion USD)	56.03	47.42	49.01	56.56
VA in transportation and mailing (Billion USD)	21.45	19.61	22.93	27.65
VA in accomodation and food (Billion USD)	11.21	10.72	9.57	6.95
VA in finance (Billion USD)	39.88	31.88	32.95	32.10
VA in real estate (Billion USD)	34.23	27.14	32.76	27.59
VA in other industries (Billion USD)	100.57	87.96	93.18	88.95
Population in 2015 (Million)	66.07	59.54	62.46	62.73
Population (Urban) in 2015 (Million)	39.46	33.01	34.63	36.17
Population (Rural) in 2015 (Million)	26.61	26.53	27.84	26.56
Employment (Urban) in 2015 (Million)	8.76	7.24	8.82	7.71
Income per person (Thousand USD)	3.37	3.89	3.25	3.78
Income (Urban) per person (Thousand USD)	4.75	5.15	4.54	5.00
Income (Rural) per person (Thousand USD)	1.78	2.22	1.86	2.02
Spending per person (Thousand USD)	2.47	2.78	2.33	2.61
Spending (Urban) per person (Thousand USD)	3.29	3.52	3.13	3.33
Spending (Rural) per person (Thousand USD)	1.49	1.79	1.47	1.54
Export + Import in 2015 (Billion USD)	316.90	137.32	165.57	132.15
Export in 2015 (Billion USD)	201.17	91.47	100.88	68.04
Import in 2015 (Billion USD)	115.73	45.86	64.68	64.11
Electricity Supply in 2015 (Billion Kwh)	220.32	238.21	246.46	294.89
Electricity Supply (Hydro) in 2015 (Billion Kwh)	67.27	113.05	9.68	1.59
Electricity Supply (Thermal) in 2015 (Billion Kwh)	128.01	120.43	223.24	273.88
Electricity Demand in 2015 (Billion Kwh)	241.82	201.97	263.30	314.68
Coke production in 2015 (Million Ton)	5.35	8.74	21.44	44.36
Crude production in 2015 (Million Ton)	11.28	0.40	12.53	15.59
Petrol production in 2015 (Million Ton)	4.52	2.84	4.14	11.43
Kerosene production in 2015 (Million Ton)	3.04	1.05	1.40	1.73
Diesel production in 2015 (Million Ton)	7.69	4.48	5.20	19.62
Fuel oil production in 2015 (Million Ton)	0.87	0.41	1.00	3.96
Natural gas production in 2015 (Million Ton)	0.45	1.24	0.77	0.13
Coal consumption in 2015 (Million Ton)	107.79	111.72	197.67	295.59
Coke consumption in 2015 (Million Ton)	7.28	11.17	19.91	38.38
Crude consumption in 2015 (Million Ton)	20.28	14.74	20.24	47.27
Petrol consumption in 2015 (Million Ton)	5.92	6.76	5.53	5.38
Kerosene consumption in 2015 (Million Ton)	1.17	1.60	0.54	0.84
Diesel consumption in 2015 (Million Ton)	8.35	7.57	6.51	8.79
Fuel oil consumption in 2015 (Million Ton)	1.46	1.79	0.75	10.90
Natural gas consumption in 2015 (Million Ton)	0.59	0.86	0.91	0.75

Note: Provinces are divided into quartile groups based on their average in-China ratio. The average for each group is weighted by province population. Economic data are sourced from the National Bureau of Statistics. Values are converted from CNY to USD using an exchange rate of 6.227.